BRNO UNIVERSITY OF TECHNOLOGY
VYSOKÉ UČENÍ TECHNICKÉ V BRNĚ

FACULTY OF CHEMISTRY
FAKULTA CHEMICKÁ

INSTITUTE OF MATERIALS SCIENCE
ÚSTAV CHEMIE MATERIÁLŮ

STUDYING THE PROPERTIES OF MOLECULAR PHOTOACTIVE MATERIALS VIA THE METHODS OF COMPUTATIONAL CHEMISTRY

STUDIUM VLASTNOSTÍ MOLEKULÁRNÍCH FOTOAKTIVNÍCH MATERIÁLŮ METODAMI VÝPOČETNÍ CHEMIE

SUMMARY OF DOCTORAL THESIS
AUTOREFERÁT DIZERTAČNÍ PRÁCE

AUTHOR — Ing. Jan Truksa
AUTOR PRÁCE

SUPERVISOR — doc. Ing. Ota Salyk, CSc.
ŠKOLITEL

BRNO 2022

ABSTRACT

In this work, the principles of theoretical density functional theory are briefly discussed first, together with the method of searching for lowest-energy structures of molecules and predicting the spectroscopic and electronic properties. Afterwards, the results of the theoretical analysis of the geometry and electronic structure of two types of molecules is presented, combined with experimental results. First, the alloxazine and lumazine, considered together as flavins, and their derivatives represent molecular materials, while adamantyl substituted polythiophenes represent polymer materials.

With respect to the flavins, different basis sets, together with the B3LYP functional, were used to find the best possible fit to experimental absorption spectra. Here, the B3LYP/6-31+G** and B3LYP/aug-cc-PVDZ methods proved to have the best correlation, with correlation coefficients 0.95 and 0.96, respectively, while the def2SVP set reached 0.94. In this context, the B3LYP/6-31+G** method seems to be the most cost-efficient. By measuring the absorption spectra of selected flavins in a mixture of dimethylsulfoxide (DMSO) and water, the spectra of flavin isomers – the alloxazine and isoalloxazine form were gained. The response of these molecules to changes in the concentration of DMSO and water will be the object of further study.

For the polythiophenes, the electronic and optical properties were theoretically investigated using model octamers, while the conformations of the adamantylated side chains were considered using trimer molecules, due to a high computational complexity. Here, the methyladamantyl thiophene was found to have a more rigid structure compared to the ethyladamantyl substituted chain, which was later confirmed *via* crystallographic analysis and atomic force microscopy scans. Crystal structures were confirmed to be present, with lattice parameters comparable to poly(3-hexylthiophene) (**P3HT**). Inspired by this research, different polymer backbones based on polythiophene were considered for future synthesis. The main recommendation here is to lower the amount of side substituents, so that only one in two or one in three thiophenes bear an adamantylated side chain.

Overall, the molecules presented here are interesting candidates for future use in optoelectronics, and the theoretical predictions generally agree with experimental results, although the comparison with experiment is not always trivial, *e.g.*, in the case of the polythiophene side chains.

KEYWORDS

Computational Chemistry, Optoelectronic Materials, Spectroscopy, Visible Light Absorption, Density Functional Theory, Alloxazine, Lumazine, Polythiophene

ABSTRAKT

V této práci jsou nejprve rychle nastíněny principy teorie funkcionálu elektronové hustoty (DFT), spolu s praktickými metodami hledání nejníže energeticky postavených struktur organických molekul a predikování jejich spektroskopických a elektronických vlastností. Poté jsou prezentovány výsledky teoretické analýzy geometrie a elektronové struktury dvou druhů molekul v kombinaci s experimentálními výsledky. Nejprve jsou diskutovány alloxazin, lumazin a jejich deriváty, souhrnně nazývané flaviny, které reprezentují molekulární materiály. Naproti tomu, struktury na bázi polythiofenu reprezentují polymerní materiály.

V případě flavinů byla nejprve nalezena nejlepší možná korelace teoretických absorpčních spekter s experimentálními na základě výpočtů se třemi různými bázovými soustavami v kombinaci s funkcionálem B3LYP. Dobrá shoda byla nalezena pomocí metod B3LYP/6-31+G** a B3LYP/aug-cc-PVDZ, které dosáhly korelačních koeficientů 0.95 a 0.96. Naproti tomu soustava def2SVP dosáhla pouze 0.94. V tomto kontextu se tak metoda B3LYP/6-31+G** jeví jako nejefektivnější vzhledem k náročnosti na výpočetní kapacitu. Měřením absorpčních spekter vybraných flavinů ve směsi dimethylsulfoxidu (DMSO) a vody byla získána spektra jednotlivých izomerů – alloxazinové a isoalloxazinové formy. Reakce těchto molekul na změny koncentrace DMSO a vody bude předmětem dalšího studia.

U polythiofenů byly studovány optické a elektrické vlastnosti na modelových oktamerech, zatímco geometrie a konformace adamantylovaných substitutentů byly z důvodu vysoké výpočetní náročnosti modelovány na trimerových molekulách. Bylo zjištěno, že thiofenový řetězec s postranními methyladamantylovými skupinami vykazuje vyšši rigiditu než řetězec substituovaný ethyladamantylem, což bylo později potvrzeno krystalografickou analýzou a skenováním povrchu pomocí mikroskopie atomárních sil. Byly nalezeny krystalické struktury s parametry srovnatelnými s poly(3-hexylthiofenem) (**P3HT**). Na základě tohoto výzkumu byly navržený nové páteřní řetězce pro možnou syntézu, jako hlavní doporučení se zde jeví snížení počtu substituentů, aby adamantylový postranní řetězec byl přítomen pouze na každém druhém či třetím thiofenu.

Zde prezentované molekuly jsou zajímavými kandidáty pro využití v optoelektronice, a teoretické predikce dosahují dobrou shodu s experimentem, přestože jejich srovnání není vždy triviální, jako je tomu například u postranních řetězců polythiofenu.

KLÍČOVÁ SLOVA

Výpočetní chemie, Optoelektronické materiály, Spektroskopie, Absorpce viditelného světla, Teorie funkcionálu elektronové hustoty, Alloxazin, Lumazin, Polythiofen

CONTENTS

1 INTRODUCTION

The field of computational chemistry has gained a great deal of interest during the past decade. Its enormous utility is based on the fact that it enables chemists to study structures that are unstable or dangerous, such as transitional states or highly toxic molecules. Furthermore, even before a new molecule is synthesized, its properties can be theoretically predicted. This possibility allows for great savings of time and money for synthetic chemists, who can gain an idea which potential molecules are worth synthesising. As such, the computational chemist may serve as a "navigator" in the synthetic effort, helping his colleagues to reach their goals at a lower cost than they would without his assistance.

First, a short overview of computational methods which are currently in use will be given, with a special focus on the density functional theory (DFT) computations. Then, the practical use of DFT in the prediction of molecular properties will be discussed in more detail. The properties of interest include molecular geometry, spectroscopic properties, and aromaticity.

Since this work is aimed at novel molecules with interesting spectroscopic properties, special attention will be paid to the prediction of different types of spectra. The most relevant type to this work is the Ultraviolet and Visible Spectrum (UV/VIS), both in the sense of absorption and emission. When discussing the spectroscopic behaviour of molecules, the effect of the solvent or solid-state interactions must be also mentioned, especially when connected to UV/VIS spectroscopy.

This work is further focused on two types of molecules – the flavins, alloxazine, lumazine and their derivatives, and polythiophenes with different side substituents. Interestingly, alloxazine and lumazine are rarely mentioned in conjunction in the literature, which motivates a detailed side-by-side study of these molecules, with the hope of creating a unified theoretical basis for their behaviour and modification These molecules have remarkable spectroscopic abilities, such as the tunability of their spectrum by the modification of the parent molecule, or by the addition on electron-donating or electron-accepting groups [1].

The polythiophenes will be theoretically investigated in terms of model octamers and trimers, due to the large computational complexity involved, especially when the large adamantylated side chains are considered. Finally, some candidates for future synthesis will be discussed, based on their geometry and electronic structure. Different uses of these materials include optoelectronics such as Organic Light Emitting Diodes (OLEDs), or photocatalysis.

2 THEORETICAL BACKGROUND

2.1 Static and Time-Dependent Density Functional Theory

The first Hohenberg-Kohn theorem states, that all properties of a molecule in the ground state are determined by the ground-state density function ρ_0. Effectively, any ground state property of a molecule is a functional of ρ_0. A functional is any rule that assigns a number to some function. Since the exact functional is unknown, an approximate energy E_0 can be obtained by using an approximate functional [2]. The second Hohenberg-Kohn theorem states, that any density function ρ other than ρ_0, commonly referred to as a trial function, will give an energy higher than the true E_0. The electronic energy from the trial function ρ_t is the energy of electrons moving in the potential field of the nuclei.

To deal with the fact that the true ρ_0 and $\mathscr{E}_0$ are unknown, the Kohn-Sham (KS) approach relies on two ideas: first, to divide E_0 into a portion which can be calculated without the functional, and a small term with the functional. This way, an error in the functional has the lowest influence on the energy. The second idea is to use an initial guess for ρ, which is then iteratively refined. Kohn and Sham have introduced a fictional reference system, in which n noninteracting electrons experience a potential field, which is chosen to make the ground-state electron probability density ρ_s of the reference system equal to the true density ρ_0.

The ground state is expressed in terms of Kohn-Sham (KS) spinorbitals ψ^{KS} [3]. The spatial parts of these orbitals can be expanded into basis functions. The selection of an appropriate basis set is a matter of balance between the accuracy and efficiency of the computation. Since the computational complexity scales rapidly (with the 4th power) with the number of individual basis functions, the set should be as small as possible. Therefore, a basis set is typically chosen to reflect the nature of the problem, such as using a diffuse basis set for ionized molecules. The most often used basis sets at currently include the Pople 6-31G and 6-311 sets [4, 5]. Further, there are the Alhrichs type sets, e.g., the def2SVP [6], often offering greater flexibility and computational efficiency than the Pople sets [7]. Finally, the correlation-consistent basis sets, such as cc-PVDZ, developed by Dunning et. al. [8], are aimed at reproducing the correlation energy of valence electrons. From here, the energy is typically determined by an iterative process using the Self Consistent Field (SCF) procedure, first proposed by Hartree [2].

In order to treat the behaviour of systems outside of equilibrium states, the time-dependent DFT (TDDFT) was developed [3, 9]. Here, initial orbitals at time t_0, $\psi_i^{KS}(\mathbf{r}, t_0)$ are found from an SCF of the static KS equation. The occupied initial orbitals are then propagated by the TD-KS equation [11]. For electronic excitations of organic molecules, the small differences between the states can be calculated using linear response theory [9].

The TDDFT method provides electronic spectra that are in good agreement with experiment, especially when close to the Frontier Molecular Orbitals FMOs [9, 10]. Furthermore, if charge transfer between two spatially separated regions is involved, range-separated hybrid functionals, and non-adiabatic approximations should be used [9].

After accounting for the mutual repulsion of nuclei, the result is a molecular energy E_{PES}, parametrically dependent on the configuration of nuclei in the system. This relationship between the energy of a molecule and its geometry is called the Potential Energy Surface (PES). Although the PES is often not explicitly shown in scientific papers, it is an essential concept in computational chemistry [1, 11]. Mathematically, the surface can be defined as a function of generalized coordinates q_1, q_2 …, q_n, which correspond to the individual bond lengths and angles. Generally, stationary points, which describe either stable structures or transition structures, are points on the geometry where derivatives of E with respect to all coordinates are zero. Stationary points, corresponding to stable molecules are energy minima, transition structures are saddle points [2, 12]. The SCF optimization is done using the Hessian, which is a matrix of second-order derivatives of E with respect to molecular coordinates.

To check whether the result is a true minimum, normal mode vibrations are used – the stretching and bending of chemical bonds where all atoms move in phase with the same frequency. Their directions and force constants can be quite easily gained by the diagonalization of the Hessian. All the force constants k are positive for a stable geometry and at least on is negative for transitive states.

Aromaticity is a key concept when describing cyclic organic compounds, especially heterocycles. Aromatic compounds are characterized by the ability to sustain a diamagnetic ring current, and many unique substitution reactions [13]. A frequently used theory-based measure of aromaticity is the Harmonic Oscillator Model of Heterocyclic Electron Delocalization (HOMHED) index. This is a geometry-based index, where the geometry of some cyclic molecule is compared to a standard. The standard should be a fully symmetrical aromatic molecule, such as benzene, with the HOMHED value of 1 is assigned to it [13].

The electromagnetic radiation in the ultraviolet and visible (UV/VIS) range has enough energy to change the electronic distribution of molecules. Here, the singlet ground state of the molecule is typically denoted as S_0. When absorbing radiation with the wavelength λ (nm), an electron is excited into a singlet excited state S_n. From here, the electron will eventually relax back to S_0, with the possibility of an intersystem crossing between S_n and a triplet state T_n. Furthermore, there is an individual PES associated with each singlet and triplet excited state. From a quantum mechanical point of view, intersystem crossings into T_n states, and internal conversions happen at intersections of the S_n excited state PES with the T_n PES and the S_0 ground state PES, respectively [14]. Deviations from experimental values are mostly caused by the interactions of the analysed molecule and solvent (*e.g.* dimethyl sulfoxide − DMSO). To deal with this, either the dielectric properties of a bulk solvent may be studied in a so-called continuum model, or several molecules of the solvent may be explicitly added to the analysed molecule during computation – this is the specific solute-solvent interaction model.

Further, the Frontier Molecular Orbital (FMO) energy levels are important for the operation of devices such as solar cells, transistors, or OLEDs. Generally, at the junction of the organic material and some inorganic electrode, the alignment of Highest Occupied and Lowest

Unoccupied Molecular Orbital (HOMO, LUMO) and the Fermi energy level of the electrode E_F decides the nature of the charge transport [15]. In solar cells and OLEDs, an interface between a p-semiconducting material and n-semiconducting material has a similar importance, so that the electron and hole from external electrodes can recombine to produce a light emission in an OLED, or that the exciton created by the light absorption of a solar cell can be split, and the electron and hole can be transported into the circuit by the conducting materials [16].

Since it is generally not possible to model polymer chains of realistic length *via* DFT, the results must be somehow extrapolated, or used indirectly, possibly to find the monomer equilibrium geometries and use them in a molecular dynamics simulation. The other option is to extrapolate results towards a limit, where the behaviour of the modelled oligomeric chain will match that of the polymer. The studied property is taken as a function of the reciprocal of the number of monomers or the number of conjugated double bonds in the backbone [17]. As the chain grows, both quantities will approach zero. Therefore, if the relationship of the HOMO/LUMO gap with one of the reciprocals can be fitted with an appropriate function, the value as the reciprocal approaches zero will correspond to the polymer HOMO/LUMO gap or other desired quantity.

The simplest possible fit – a linear function – often fails to predict the behaviour of polymers, where the relation of excitation energy to length saturates for long chains [18]. In the case of the HOMO/LUMO gap, a two-parameter model described by Kuhn, involving the electronic excitation energy, the energy of a single double bond, and a relative force constant, measuring the coupling of single and double bonds [19] has proven quite efficient [18, 20]

2.2 Alloxazine Chemistry

Alloxazines, commonly also known as flavins, are derivatives of the tri-cyclic benzo[g]pteridine-2,4-dione, which is itself based on the parent molecule lumazine (see **Fig. 1**), although lumazine itself typically is not considered to be a part of this family [21]. Alloxazine-type molecules have long been known as efficient chromophores [22]. Presently, these molecules are considered for use in bioorganic sensing and optoelectronics, highlighted by Golczak [23], who has used the **AL** molecule with an additional fused benzene ring for a study of human red blood cells with fluorescence microscopy. There are useful in the field, because of the great tunability of their spectroscopic properties, and the ability to be incorporated into DNA [1]. Lumazine is a part of the metabolic pathways of flavins, such as the biosynthesis of riboflavin [24]. Due to the structural similarity, the possibilities for the application of lumazine are almost the same as for **AL**.

The use of substituted Flavins as photosensitizers may also have a biological significance in the context of photoantimicrobial therapy, where *e.g.*, riboflavin has been proven to be able to convert oxygen from the triplet state into singlet, which then kills bacteria due to its strong oxidative properties [25]. However, even non-biological oxidations can be considered, e.g. the preparation of sulfoxides from sulphides via an Alloxazine molecule, amidated at the N(3) position [26].

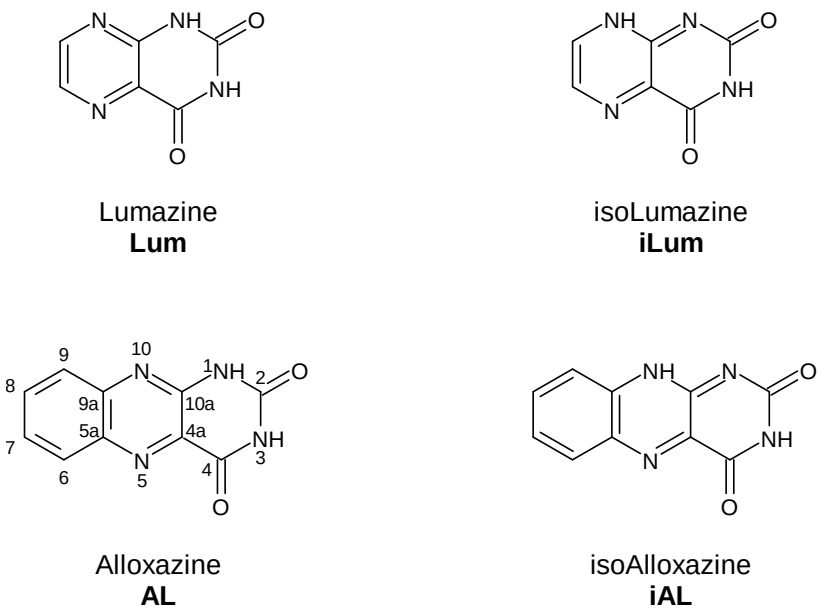

Fig. 1 *The structures and isomers of alloxazine and lumazine*

Furthermore, these molecules undergo isomerisation, which amounts to the transfer of a proton from N(1) to N(10), see **Fig. 1**. This leads to a noticeable red shift of about 50-100 nm [21] in the absorption and fluorescence spectrum. In aprotic solvents, this process is not expected to happen [27], though absorption peaks, which could correspond to **iAL**, have been found in the dimethyl sulfoxide (DMSO) solvent [28]. Whether the **iAL** form could be present due to trace amounts of water in the DMSO, or if there is a different, aprotic, isomerisation mechanism is still up to discussion, although a water-facilitated mechanism is generally considered in the literature [29].

In the case of lumazine, the same basic isomerization is reported as in alloxazine, although the red shift is often ascribed to an N(1) or N(3) deprotonated form, present in neutral and basic solutions [30], while there is expected to be a minority population of the **iLum** form [31]. Interestingly, studies of **AL** are focused on the N(1)–N(10) tautomers, while studies of **Lum** mostly consider ion forms. Recently the presence of an ionic form has been confirmed for lumazine [32], while no such study supports the photo-induced deprotonation of **AL**.

Choudhury et. al. [33] have pointed out a red shift in solvents that consist of acetonitrile (ACN) and water, and dimethylformamide and water mixtures, the absorption spectrum consistently shifts into higher wavelengths, and an isoalloxazinic peak appears in the emission spectrum. They have theorized, that this behaviour could be used to monitor the local solvent concentration in the space around the Flavin molecule. Indeed, since then, the role of the pteridine moiety in tyrosine-kinase inhibitance has been successfully described [34], using fluorescence spectroscopy in an ACN–H_2O mixture of varying concentration.

From the computational point of view, some groundwork was laid by Salzmann, Sikorska and Kabir [35–37]. They have investigated the electronic excited states both in a vacuum and in an

implicit and explicit water solvent. They have found, that to fully account for the solvatochromism of the two absorption peaks of **AL** and **Lch**, a combination of implicit and explicit models is needed, requiring 4-6 H_2O molecules to fully account for solvation in water. However, both the studies of Kabir and Salzmann [35, 37] focus only on the parent **AL** and the extremely simple derivative **Lch**, without even considering the isomerization. This leaves them open to the question, how does their model account for other derivatives, and whether such complexity is truly needed.

By investigating Alloxazine-water complexes, Mal et. al. [38] have concluded, that the tautomerization is linked to the motion of the assisting H_2O molecule, and to a large extent driven by the solvation dynamics of water. Furthermore, they found that most of the proton transfers occurs in the excited state, due to a significantly lower energetic barrier, which was already observed as phototautomerism [39]. This observation could lead to a general description of Flavin isomerization, independent of the solvent.

North et. al. [40] have concerned themselves with simple asymmetrical substitutions in the C(7) and C(8) positions, i.e., using different substituents on C(7) and C(8) in every molecule. They have predicted that electron-donating substituents, such as $–CH_3$, lead to a more even distribution of the HOMO orbital and a substantial bend along the imaginary axis formed by N(5) and N(10), which correlates with their Mulliken atomic charges. Electron-withdrawing substituents, e.g., –CN have the exact opposite effect, resulting in a planar molecule and frontier MOs localized on individual atoms.

Afaneh et. al. [31] have performed an extensive study of the lumazine structure in neutral conditions. They have considered many possible isomers, including protonated oxygens. By ordering them in terms of relative energy, they have found that the **Lum** form as shown in fig. 4 is the lowest, followed by **iLum**, around 8 kJ mol^{-1} higher. Forms with protons on the C(2)=O and C(4)=O oxygen atoms are around 40 kJ mol^{-1} higher. It follows that a majority presence of **Lum** can be expected in pH-neutral water or aprotic solvents, along with a smaller population of **iLum** or an anion in water. In acidic environments, the **Lum** form is expected exclusively, with an addition of N(1) and N(3) deprotonated anions in alkaline solutions [30, 31].

A wealth of information exists on the structural modifications of lumazine, unfortunately often focused on purely biological descriptors such as antibacterial activity [41], which makes a comparison with the photophysics of **AL** modification impossible. Due to the similarity of the two molecules, it could be assumed that most modification strategies can be carried over from alloxazine, however, computational chemistry could provide at least a limited insight here. For example, substituents in the C(6) and C(7) positions of **Lum** should have a stronger effect on the electronic structure, since they are not shielded from the heterocyclic moiety by an additional benzene ring as is the case in C(7) and C(8) substituted **AL**. Indeed, the strong electron-withdrawing group –CN has a much larger effect on **Lum**, than other such groups have on **AL**, leading to a substantial red shift in spectra and increased acidity of the N(1) proton [42].

2.3 Polythiophene Chemistry

Polythiophene-based materials are used in the fabrication of devices such as OLEDs, Organic Field Effect Transistors (OFETs), Organic Photovoltaic Cells (OPVs) or sensors since they are efficient semiconductors with well-known optical properties. Their main advantages lie in the low production cost and synthetic flexibility. Indeed, by modifying the molecule, it is possible to tune the solubility, structure, and electrochemical properties [43]. A basic structure of polythiophene (**PT**) is shown in **Fig. 2**. Furthermore, the sulphur atom on a thiophene ring contributes to the molecular aromaticity and allows the formation of intermolecular S–S and S–O weak bonds, due to the lone pair electrons in 3s and 3p orbitals [43]. Obviously, **PT** has the capacity to create organised solid-state structures even without any modifications, which makes it a prime candidate for use in optoelectronics. Finally, the quinoid resonance structure (**see Fig. 9**) of thiophene oligomers and polymers features higher rigidity and lower band gap, although it is higher in energy.

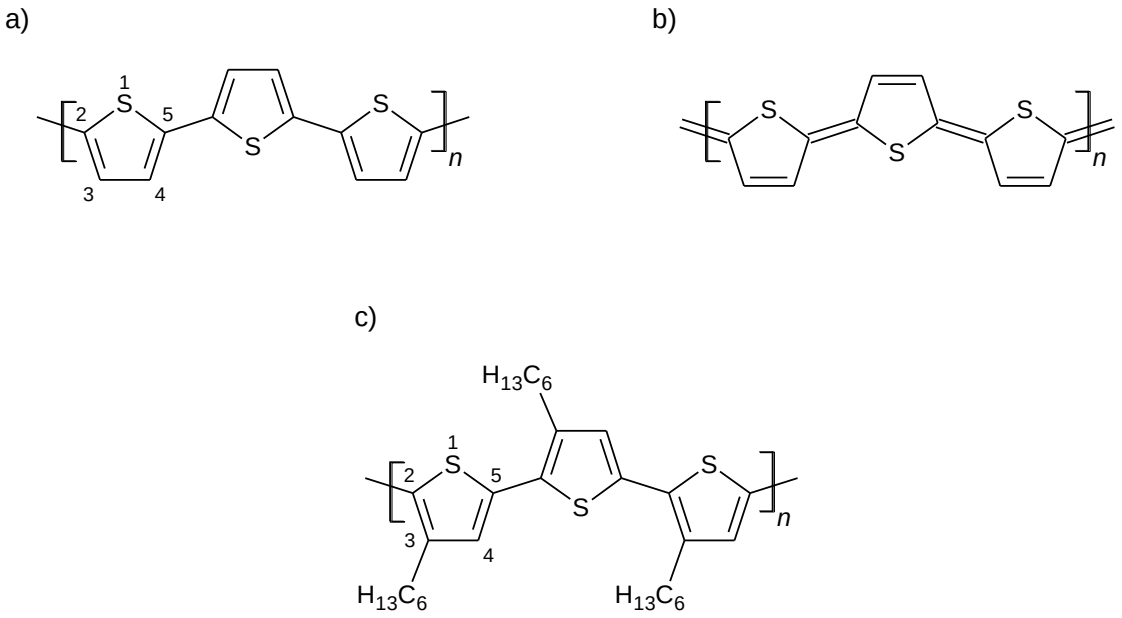

Fig. 2 *The structure of polythiophene: a) the aromatic form and the numbering of the thiophene moiety; b) the quinoid form; c) poly(3-hexylthiophene), the most common substituted* ***PT***

Unsubstituted oligothiophenes are p-type semiconductors with a comparatively low charge carrier mobility, below 0.1 $cm^2\ V^{-1}\ s^{-1}$. This can be raised substantially by ending the chain with alkyl groups in the C(2) and C(5) positions on the ends of the oligomer chain. Fluoride-substituted benzene was found to have a similar effect. In this way, the mobility rises to 0.6 $cm^2\ V^{-1}\ s^{-1}$ [44]. The thiophene dimer absorbs visible light around 300 nm and has an emission band around 360 nm. The addition of thiophene units to the chain causes a red shift due to higher conjugation, and a substantially larger fluorescence quantum yield. Once over 25 thiophene units are present in the chain, the absorption and emission wavelengths stabilize at 450 nm and 650 nm, respectively.

While the systematic studies of the side chain influence on thermal stability started relatively recently, Cao et. al. [45] have explored the effect of different linear and branching alkyls and have found that by placing the branching point closer to the backbone, both melting point and glass transition temperature are increased as a result of tighter molecular packing in the side-chain direction. For an illustration of substituted **PT** packing, see **Fig. 3**. At the same time, Schaffrinna et. al. [46] have investigated the optical properties of substituted **PT**s, and have managed to create a significant blue shift of around 100 nm, both in solution and in a thin film, by substituting acetic acid in the C(3) position. This material also exhibited good adhesion to the polar surfaces due to packing in the edge-on direction (**see Fig. 3**).

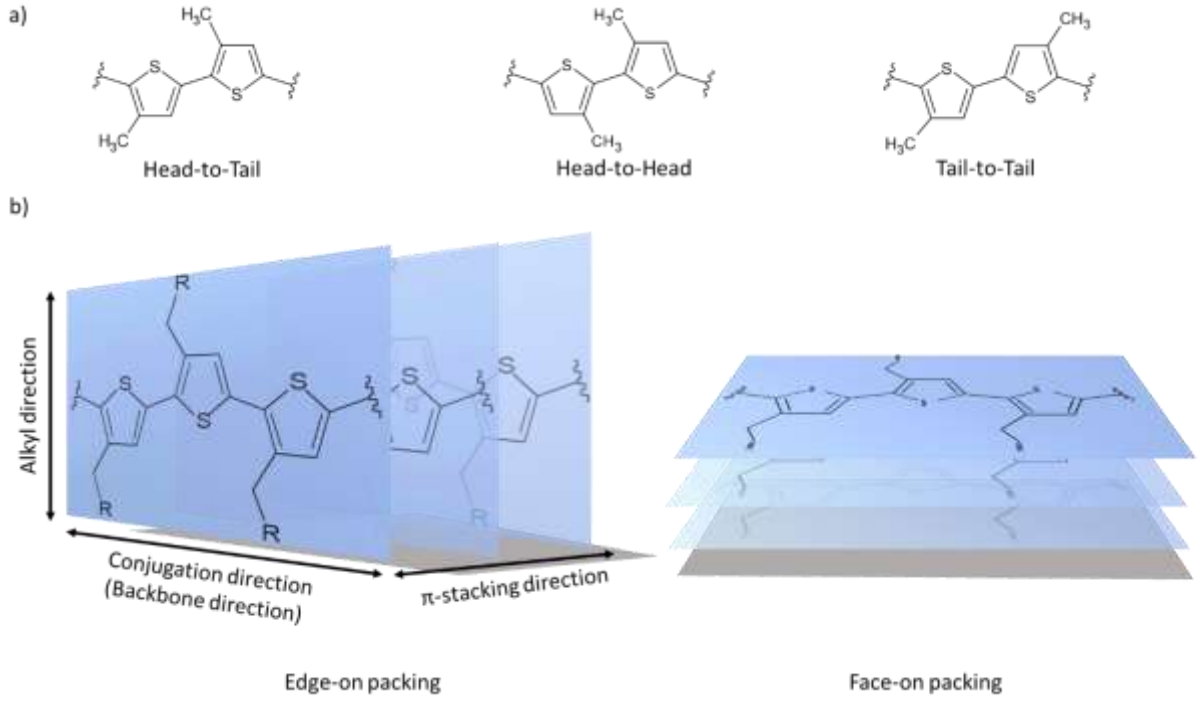

Fig. 3 *a) Possible regioregularities of substituted polythiophenes; b) An illustration of the possible packing of side-chain substituted polythiophenes in relation to the substrate (grey surface) [43]*

Perhaps the most used molecule of the polythiophene class is the hexyl-substituted poly(3-hexylthiophene), denoted **P3HT**. It reaches charge carrier mobilities of around 0.2 $cm^2\ V^{-1}\ s^{-1}$ when in the edge-on orientation and head-to-tail regioregularity (see **Fig. 3**). On the other hand, other the head-to-head and tail-to-tail arrangements cause torsion in the structure, thus lowering the overall conjugation and charge mobility. The absorption and emission bands of **P3HT** are located around 450 nm and 550 nm, respectively, while in solution. Deposition into thin film leads to a red shift of around 50 nm in absorption, and 200 nm in emission.

Since the favourable conductive properties of **P3HT** stem largely from its packing [47], a viable strategy to further improve the crystallinity and π-stacking of **PT**s could be side chain engineering. Some groundwork has been laid by Nguyen et. al. [48], who have synthesized

poly(3-alkylthiophenes) (**P3AT**s) with butyl, hexyl, and octyl side chains, with well-defined molecular weights (MWs). Subsequent analysis has revealed that larger alkyl chains lead to higher crystallinity, and optimal performance in OPV cells, which was likely caused by the higher degree of crystallinity. On the other hand, the side chains proved to have only a small influence on the position of optical absorption and emission bands, whereas the length of the main chain, characterised by MW, had a much greater influence. This is hardly surprising, since the spectroscopic properties are mainly a function of FMO energy levels, which are not influenced by alkyl substitution very much, and side chains with some heteroatoms would need to be used.

While current research focuses on different linear and branched molecules, there is a lack of studies performed with a large, three-dimensional substituent, such as adamantane. This molecule is stable, biocompatible, and readily self-organizes into crystals [49]. In the past, this substituent has been used to enhance the crystallinity and hole mobility of molecular materials such as **PP**s, without compromising their spectroscopic properties and fluorescence quantum yields. In fact, adamantyl substitution was found to induce crystallization in long, needle-like structures, that are around 1 μm long [49]. Thus, it represents unexplored opportunities in side-chain engineering.

Although DFT methods are not yet able to give precise insight into polymer molecular packing, some information, especially about the intramolecular effects can be extracted from computations carried out on oligomers. Already in 2004, Marcon et. al. [50] used *ab initio* intramolecular torsional potential and charge distribution of 6–membered oligomers (sexithiophenes) to obtain a better fit of the molecular mechanics force field. By using these more advanced parameters, they managed to obtain a theoretical crystal structure of sexithiophene and fluorinated sexithiophene that were in good agreement with the experiment.

Later, Darling et. al. [51] addressed the question of the polymer limit – how many thiophene units are needed for a DFT model to be accurate for a polymer chain, especially when the side chains are treated explicitly. While the alkyl side chains do not participate in forming FMOs, and thus do not directly contribute to light absorption, they are extremely important for crystal packing and therefore the conductivity of **P3HT**, and it is difficult to imagine a successful model of side-substituted **PT**s that does not explicitly treat them. Furthermore, the side substituents affect the dihedral angles between thiophene units, thus contributing to the conjugation in the backbone. The study of Darling was especially focused on dihedrals and has determined, that 8–10 thiophene units provide a good approximation for the **PT** chain, while there are only negligible differences between the torsional potential profiles of 10- and 14-unit **P3AT** chains. Indeed, the global minimum of torsional potential is around 150 ° for dimer thiophene, and 180 ° for an octamer and higher. This behaviour is attributed to the increasing electron dislocation in longer chains, which makes deviations from a planar conformation less energetically favourable [52].

3 AIMS OF THE THESIS

Apart from giving an overview of the DFT method and its practical use, this work mainly aims to investigate the properties of the two types of molecules mentioned above, especially to see whether they could find some use in the field of optoelectronics.

Concerning the flavin class of molecules, the first aim of the research is to develop a consistent model of their spectroscopic behaviour based on existing experimental data from our own research, and from literature. This model could then be used to predict the behaviour of possible synthesized molecules, and to pick the most suitable candidates for a given application in optoelectronics, for instance, information such as the FMO energies and the HOMO/LUMO gap can be used to determine possible candidates for OPVs or other areas like photocatalysis.

Further, it should be possible to find some insight into the molecular structure, *e.g.*, by investigating the geometrical distortion caused by different substituents, that could be useful for further synthesis.

Since the topics of **AL** and **Lum** chemistry are so rarely mentioned together, it is a further goal to determine, whether a coherent model could be prepared for both of these classes simultaneously. On the other hand, deazaflavins have been shown as too different in reactivity (see the beginning of chapter 3.1, or ref. [21] for details), and it is doubtful that they fit the same chemical space, i.e. that a model made for alloxazine would fully fit them. Furthermore, there is significantly less data on the photophysics of deazaflavins in the literature, essentially all of it being done by the group of Sikorski [23], and no samples were available for this work, since the synthetic route is different [53].

In the case of the thiophene derivatives, the main aim was to theoretically investigate the influence of the novel adamantyl side substituents on the properties of **PT**, especially with regards to the possible conformations of the side chains with respect to the backbone and sterical effects, which could provide some insight on the possibility of intermolecular packing in the side chain direction. As before, the FMO energy levels and spectroscopic properties will be important.

4 METHODS OF RESEARCH

4.1 Calculation

In the case of DFT studies of flavins, the three-parameter hybrid B3LYP functional [54] was used, together with the 6-31+G**, aug-cc-PVDZ [55] and def2SVP [56] basis sets to compare their results and create a meaningful model. Tight optimisation criteria were set for the computation, with a large DFT integration grid. For molecules with freely rotating substituents, the lowest energy conformation was found first *via* a relaxed PES scan. Computations were done by first stabilizing the gas phase geometry, and then using the PCM model [57] for minor alterations. Later, the vertical singlet transition energies and oscillator strengths between the initial and final electronic states were computed by the TDDFT method using the B3LYP functional. Excited state geometries and deexcitation energies were found by the same method. True minima on the potential energy surface were confirmed by an inspection of the frequencies for all geometry stabilizations.

For future reference, the molecules considered in the flavin-focused part of the study are shown in **Fig. 4**, where the molecules drawn in bold black lines have been previously prepared and characterised – and so they can be compared to experimental results. The molecules drawn in thin grey lines are not available for synthesis at this time. Further, the A, B, and C notation for the individual rings of the **AL** and **Lum** moieties is introduced, useful for describing structural changes caused by different substituents by the HOMHED index.

For the computations on **PT** and its derivatives, the B3LYP/def2SVP method was used. For the sake of simplicity, calculations were performed in the gas phase. As before, the optimisation process was performed by tight optimisation criteria and a large DFT integration grid. True minima on potential energy surface were confirmed for small model molecules through vibrational analysis by no imaginary frequencies check. The minimum-energy geometries were found for model octamers and trimers of the molecules in **Fig. 5**. Two all-*trans* arrangements were considered for all molecules since *cis* conformations are not preferred in unsubstituted and alkyl-substituted **PT**s due to sterical repulsion [58]. One of the two considered orientations was the *syn*-conformer, with positive values for all dihedral angles between thiophene rings, which gives it a spiral shape. The second was the *anti*-conformer, with alternating positive and negative values of the dihedrals.

Once the lowest-energy geometries were found, the vertical transition energies and oscillator strengths between the initial and final electronic states were computed by the TDDFT method. The trimer calculations were focused on finding the potential energy profile of rotation around the dihedral angle between the thiophene chain and its substituent, this was performed by a relaxed PES scan across the whole range of rotation, with a 20° step and a finer 5° step scan at the energy maxima. This part of the study was performed only for the (**3HT**)$_3$, (**MAT**)$_3$ and (**EAT**)$_3$ trimers, since the relaxed PES scan is very resource and time intensive, and it did not seem to make sense to perform it for the other substituted molecules that only exist in theory.

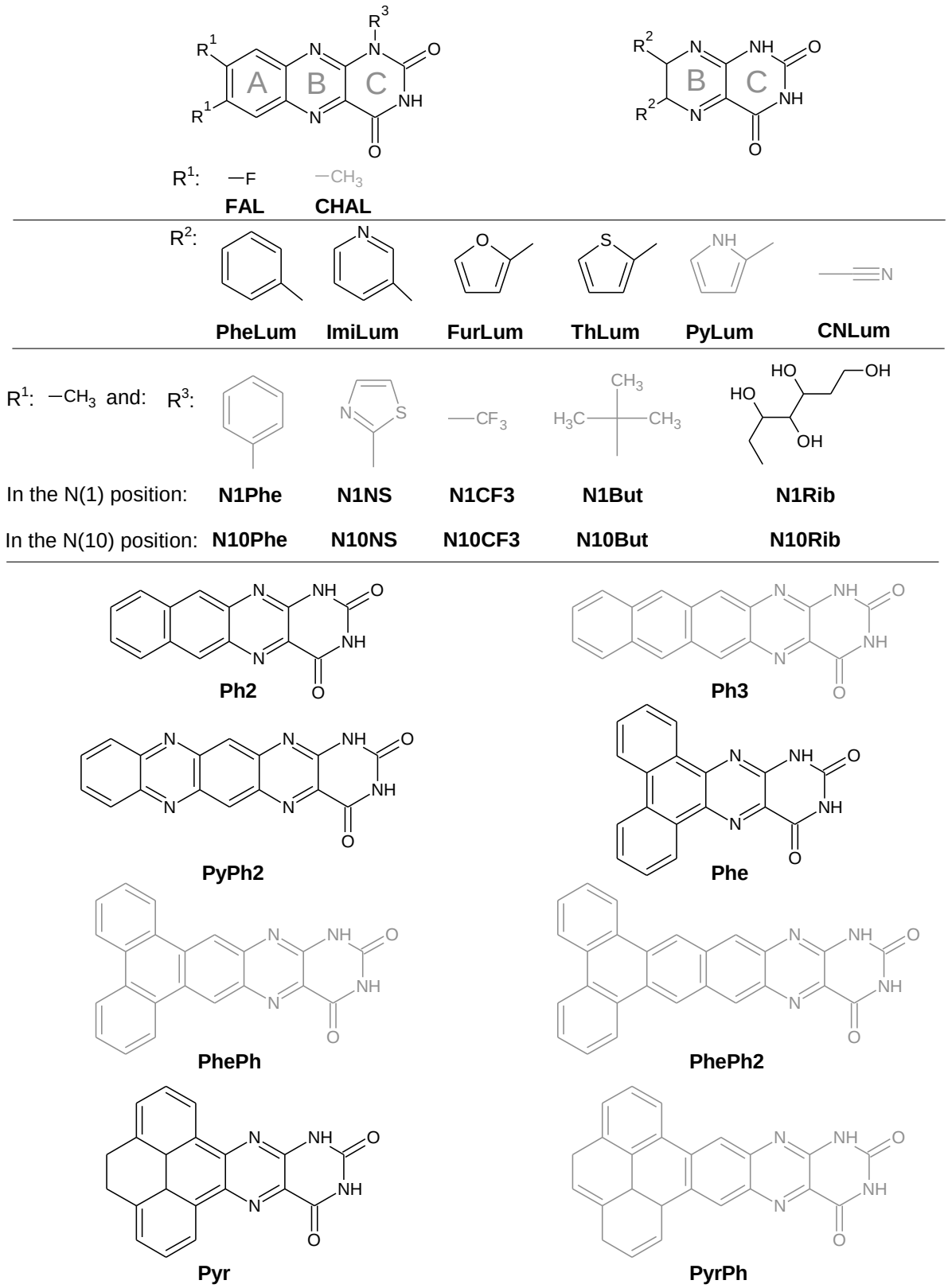

Fig. 4 *The **AL** and **Lum** derivatives considered in this work. The molecules where relevant experimental data is available are printed in black, ones that are purely theoretical are grey. The A, B, C ring notation of alloxazine and lumazine is also shown. While the **CHAL** molecule is widely used, spectroscopic data in DMSO is not available at this time. Isoalloxazine forms are not pictured but are included in the study.*

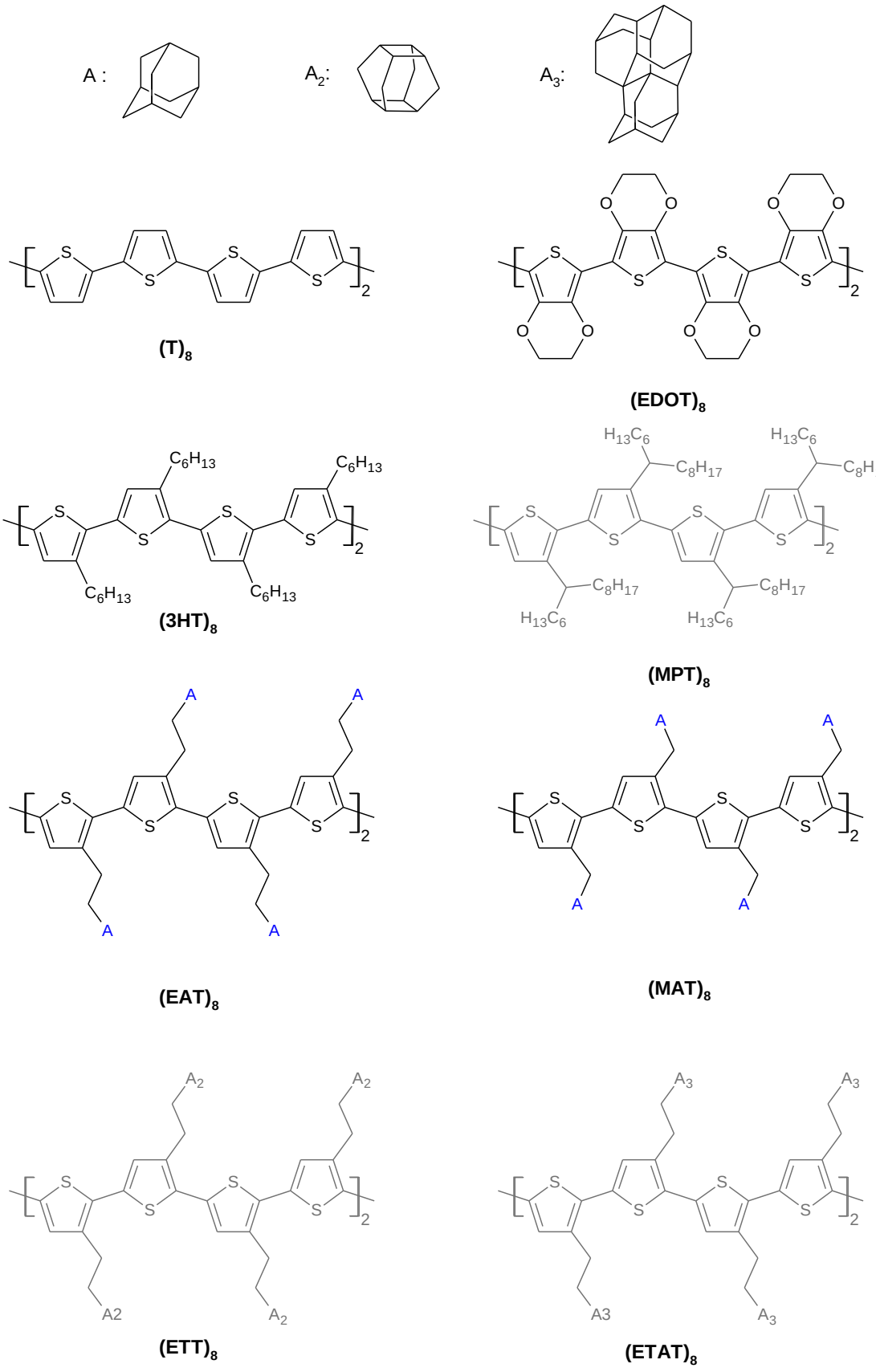

Fig. 5 *The structures considered in the study of adamantylated thiophenes [JT3]. The trimers are not pictured.*

4.2 Experimental

The absorption spectra were measured using a Specord 50 Plus UV-Vis spectrophotometer (Analytik Jena, Jena, Germany). Emission measurements were done using a Horiba Fluorolog (Horiba Jobin Yvon, Kyoto, Japan). The concentration of all samples was 1 10^{-5} mol l^{-1}. The baseline for the spectra was determined by measuring the absorption of the solvent, either pure DMSO (purchased from Honeywell Research Chemicals, 99.9 % purity, maximum 0.02 % water content [59]) or the appropriate DMSO-H_2O mixture. A Hellma QS quartz cuvette with an optical path of 1 cm was used for the optical measurements. All experiments were performed at room temperature, while deionized water with the conductivity of 0.06 μS cm^{-1} (prepared in-house at the Faculty of Chemistry) was used to dilute the samples when needed.

The molecules studied by this method were **Lum**, **AL**, **FAL**, and **ImiLum**. The **Lum** molecule was supplied by the BDL Czech Republic at > 99.0 % purity, and other measured samples were prepared according to the work of Richtar et al [28], and generously donated by dr. Richtar.

Further, the molecules **Ph2**, **PyPh2**, **Phe** and **Pyr** were measured in DMSO only, at the same concentration and room temperature. Other measurements, such as the heterocycle-substituted lumazines were taken from literature or the previous work of this group, such as [28]. The DMSO used in this part contained a larger fraction of water (Penta Chemicals, max. 0.3 % water content [60]), and the samples can be expected to contain both isomers.

Atomic Force Microscopy (AFM) was performed on thin layer samples of **P3HT**, and the newly prepared **PEAT** and **PMAT**. The AFM scans were done using a Burker NanoWizard microscope in the noncontact mode using the TESPA V2 cantilever. After the measurement, an automatically determined baseline was subtracted from all scanned lines to account for the internal vibrations of the cantilever. The samples for measurement were prepared by spin coating a thin layer of the polymer in question onto an Indium Tin Oxide (ITO)/glass substrate at 3000 revolutions per minute (rpm) for 60 seconds with a 30 s pre-spin at 1500 rpm. The chloroform solutions for spin coating had the concentration of 10 mg ml^{-1}.

4.3 Software

To carry out the computations described above, the Gaussian 16 [61] program package was used, allowing for the simple use of a plethora of functionals and basis sets, with the corresponding corrections, e.g., range correction or empirical dispersion. The absorption spectra recording was done via the ASpectUV [62] program, provided by the manufacturer of the spectrometer. Similarly, the fluorescence measurements were recorded and processed using the FluorEssence [63] software. The computations were carried out with the use of the Metacentrum VO [64] infrastructure. For the visualisations of molecular geometries, molecular orbitals and dipole moments, the Avogadro [65] and Molekel [66] freeware program packages were used. For processing the computational results and measured data, the MS Excel and Origin 2019 proprietary packages were used.

5 RESULTS AND DISCUSSION

5.1 Flavins structure and spectroscopy

In **Tab. 1**, the dihedral angles γ_1, γ_2, and δ of these conformations are given, as shown in **Fig. 6**. The angles γ_1, and γ_2 are always taken from the C atom opposite to the heteroatom, to take the asymmetry of heterocyclics into account. Thus, when both γ_1 and γ_2 have a positive or negative value, the molecule is arranged symmetrically, while if they do not have the same sign, the molecule is asymmetrical. Further, molecules which have the heterocyclic substituents close to a planar arrangement cause a large distortion of the B ring, indicated by the τ dihedral.

Further, the isomerisation introduces asymmetry into many of the **Lum** derivatives, as one of the heterocycles interacts with the N(10) hydrogen, and the other possibly increases the angle γ_2, in order to compensate for the distortion of the central moiety. On the other hand, the hypothetical **PyLum** derivative is the closest to a planar structure, but at the cost of a very large strain on the central rings.

Finally, the substituents in the N(1) and N(10) positions of CH have a dihedral δ dependent on their structure, with But and CF3 preferring a non-eclipsed conformation, and the planar phenyl and thiazole prefer a 90 °angle. The ribityl chain in N(1) interacts with the C(2)=O group, which leads to a large change in structure versus the typically encountered riboflavin **N10Rib**. Further, with large substituents such as But and CF3, a bending of the isoalloxazine moiety is observed, as previously shown by North [40]. It seems that a pyramid-shaped substituent directly bound to N(10) is required to induce this effect since it is not present in **N10Rib**, **N10Phe** or **N10NS**.

The native **AL** molecule shows a high degree of aromaticity, with the HOMED index being 0.94, 0.93 and 0.83 for rings A, B and C, respectively. The isomerisation brings about a decrease in aromaticity, with **iAL** having the values 0.98, 0.87 and 0.68 in the three rings, obviously caused by the double bond shifting from ring B to ring C. Binding substituents in the N(1) or N(10) position decreases the aromaticity of the C and B ring respectively, due to deforming the rings, especially in the case of large three-dimensional substituents like CF_3 [JT2]. Interestingly, as more benzenes are fused to the A ring, the aromaticity also generally decreases, showing that the A ring geometry deviates from benzene [JT1].

Next, statistically significant fits of the experimental and predicted values have been by the procedure described above. The CAM-B3LYP functional was abandoned early on, as it proved to have the worst fit. **Figure 7** shows the linear regression of the fits described above, for the best performing basis set – aug-cc-PVDZ – in terms of the wavelengths and energies. The fits of the other methods are summarized in **Tab. 2**. Further, there is a slight discrepancy between the energy and wavelength fits, as seen in **Fig. 7** this is likely caused by the computational errors introduced by converting the experimental wavelength data into energy values. Generally, the fit is slightly worsened by adding the **Lum**-type molecules, especially their iso forms, due to the inconsistency in underestimating **iAL** peaks, while overestimating substituted **iLum** peaks.

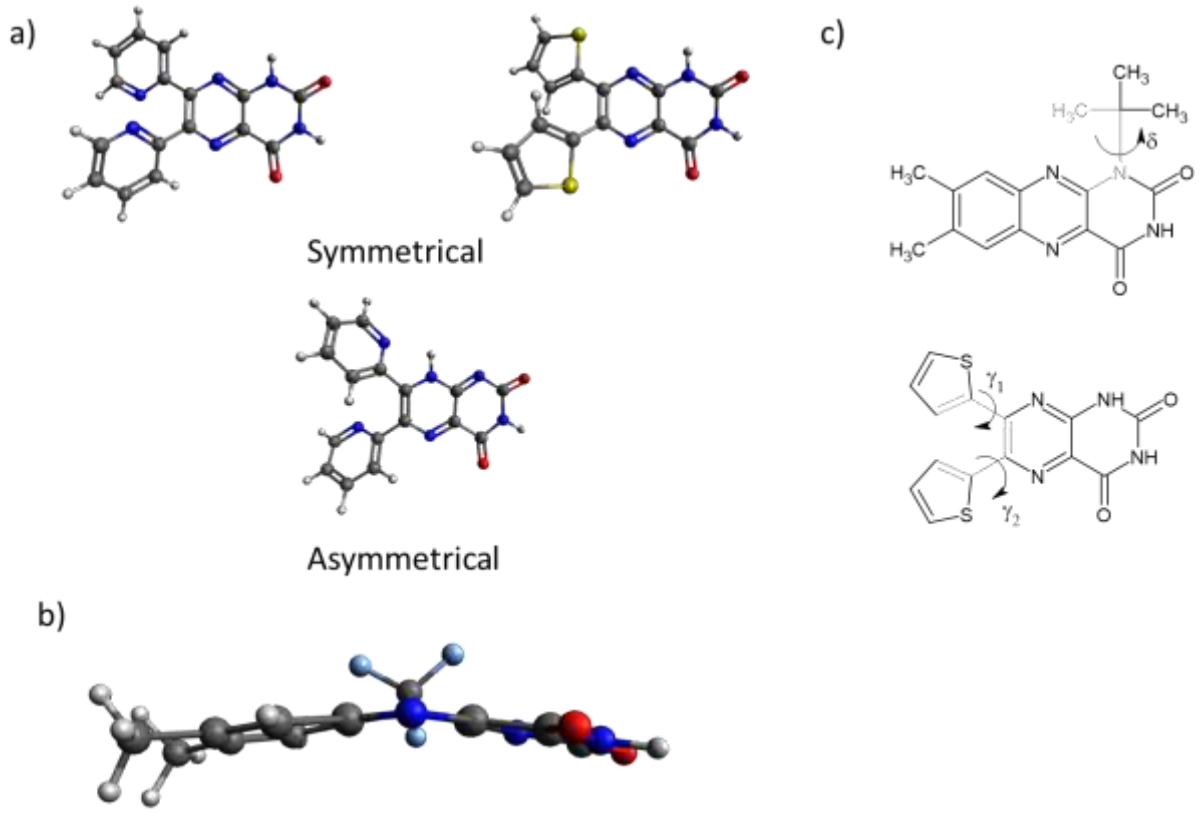

Fig. 6 *a) the symmetrical / asymmetrical arrangement of the lumazines, where yellow atoms are sulfur, blue atoms are nitrogen, and red atoms are oxygen; b) the structural bend of the B ring, observed with butyl and CF_3 substitutions into the N(10) position.*

Tab. 1 *the dihedral angles of the lowest-energy configurations in the heterocycle-substituted* ***Lum*** *and the N(1) and N(10) substituted* ***CHAL****. Due to the negligible differences across basis sets, only def2SVP values are given.*

Molecule	γ_1 (°)	γ_2 (°)	τ (°)	Molecule	δ
PheLum	-149.089	-140.049	8.524	**N1But**	38.831
iPheLum	-135.309	-140.95	5.115	**N10But**	-123.206
ImiLum	145.013	149.624	-8.409	**N1CF$_3$**	60.001
iImiLum	28.396	-157.221	7.618	**N10CF$_3$**	79.495
PyLum	24.997	15.212	26.961	**N1NS**	100.008
iPyLum	14.725	13.822	24.977	**N10NS**	97.083
FurLum	-23.457	156.349	-9.174	**N1Phe**	82.198
iFurLum	-22.05	176.174	-6.438	**N10Phe**	89.502
ThLum	-24.741	-35.007	-10.899	**N1Rib**	63.192
iThLum	48.24	26.096	4.746	**N10Rib**	-75.045

.

The def2SVP fit line is the closest to $y = x$, meaning the values are accurate, but lack precision, and have a larger spread than the other methods. At the same time, the aug-cc-PVDZ basis set has the greatest overestimation, which may be caused by overestimating the degree of π-conjugation, thus calculating the orbital gaps too low. Outliers from this basis set, are the **iPh2** $S_0 \rightarrow S_2$ transition, the **iPyr** $S_0 \rightarrow S_1$ transition, and the **iF** $S_0 \rightarrow S_4$ transition. There are visible aggregates in **Fig. 7**, especially around the y = 300 nm and y = 280 nm lines. This is caused by reading values from experimental spectra, where the absorption band at 280–300 nm is often not clearly resolved, and multiple molecules get this wavelength assigned due to experimental imprecision. Therefore, deleting the iso-forms from the dataset automatically improves all fits, since these ambiguities are partly removed. Finally, the cluster seen around the y = 450 nm line is the product of underestimating the $S_0 \rightarrow S_1$ transition of isoalloxazine isomers.

Due to the broad fluorescence bands, and the fact that the method in this work was optimized for ground-state molecules and absorption predictions, the predicted emissions do not correlate satisfactorily with the experiment. However, there is at least a qualitative agreement, especially for the aug-cc-PVDZ basis set. Interestingly, while the calculations typically underestimate the **iAL** and **iLum** absorptions as seen above, the opposite is true in the case of heterocyclic substitution. Otherwise, the theoretical predictions are within 30 nm of experimental values, which is an acceptable outcome concerning the SCRF model.

Finally, a brief overview of the energy levels is now presented, accompanied by an illustration in **Fig. 8**. The results of the two well-performing basis sets, 6-31+G** and aug-cc-PVDZ, have been selected for this part. Generally, the isoalloxazine / isolumazine form has a smaller HOMO/LUMO gap, as predicted by Chang [67]. The large conjugated **Ph2**, **Ph3**, and **PhePh2** molecules appear to be exceptions to this rule, although there is no experimental confirmation currently and available measurements [28, 23] do not indicate this to be the case for **Ph2**.

Further, the strong electron-withdrawing group seems to have a profound effect on **Lum**, with the gaps of **CNLum** being around 0.4 eV lower than those of **Lum**. On the other hand, the energy levels of **FAL** remain essentially unchanged w.r.t. **AL**. Substituents in the N(1) or N(10) positions have very little effect on FMOs, except for $–CF_3$, which lowers the **iAL** gap by around 0.1 eV. The effect of these substituents would likely have been bigger if they contained a heteroatom bound directly to the N(1) or N(10) positions. As the conjugated system grows, the HOMO/LUMO gap predictably decreases, and in the extreme case of very large molecules such as **PhePh2**, it is lowered by around 1.5 eV w.r.t. the parent molecule **AL** or **iAL**. On the other hand, substituting heterocycles in the C(6) and C(7) positions of **Lum** consistently lowers the respective HOMO/LUMO gaps by around 1.5 eV. In this context, both enlarging the fused system, and substituting freely rotating rings seem to be valid design strategies for tuning the electronic structure of the molecules.

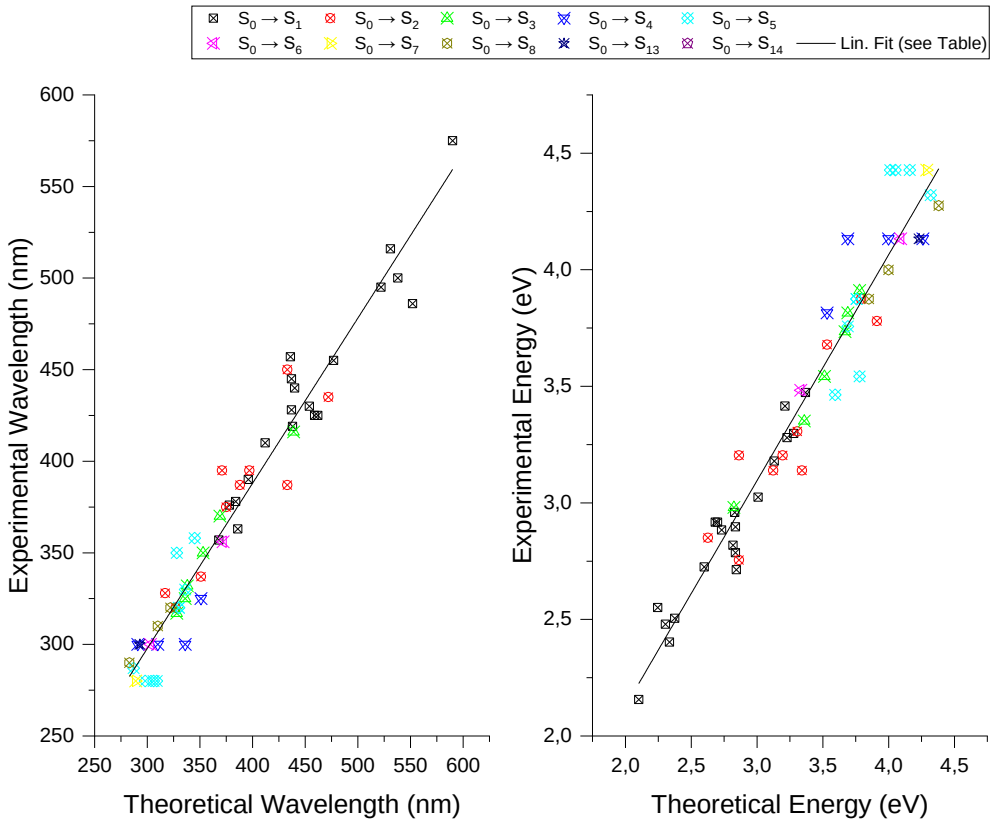

Basis set	aug-cc-PVDZ	aug-cc-PVDZ No iso forms
Linear Fit (Wavelength, nm)	$\lambda_{exp} = 0{,}902 \cdot \lambda_{teor} + 27{,}253$	$\lambda_{exp} = 0{,}920 \cdot \lambda_{teor} + 20{,}526$
R	0,951	0,970
Linear Fit (Energy eV)	$E_{exp} = 0{,}969 \cdot E_{teor} + 0{,}189$	$E_{exp} = 0{,}961 \cdot E_{teor} + 0{,}214$
R	0,944	0,952

Fig. 7 *The obtained linear dependences for the 6-31+G**, def2SVP, and aug-cc-PVDZ computations, in terms of both wavelength on the left and energy on the right.*

Tab. 2 *The summary of the linear fits of CAM-B3LYP/6-31+G** and B3LYP/def2SVP theoretical and experimental spectra.*

Basis set	CAM-B3LYP/6-31+G**	6-31+G** No iso forms
Linear Fit (Wavelength, nm)	$\lambda_{exp} = 1{,}366 \cdot \lambda_{teor} - 85{,}686$	$\lambda_{exp} = 0{,}970 \cdot \lambda_{teor} - 105{,}197$
R	0,876	0,825
Linear Fit (Energy, eV)	$E_{exp} = 1{,}032 \cdot E_{teor} - 0{,}460$	$E_{exp} = 1{,}110 \cdot E_{teor} - 0{,}759$
R	0,839	0,786
Basis set	def2SVP	def2SVP No iso forms
Linear Fit (Wavelength, nm)	$\lambda_{exp} = 0{,}990 \cdot \lambda_{teor} + 1{,}840$	$\lambda_{exp} = 1{,}079 \cdot \lambda_{teor} - 25{,}442$
R	0,948	0,954
Linear Fit (Energy, eV)	$E_{exp} = 0{,}991 \cdot E_{teor} + 0{,}051$	$E_{exp} = 1{,}054 \cdot E_{teor} - 0{,}204$
R	0,936	0,933
Basis set	6-31+G**	6-31+G** No iso forms
Linear Fit (Wavelength, nm)	$\lambda_{exp} = 0{,}919 \cdot \lambda_{teor} + 25{,}638$	$\lambda_{exp} = 0{,}970 \cdot \lambda_{teor} + 8{,}704$
R	0,951	0,953
Linear Fit (Energy, eV)	$E_{exp} = 0{,}953 \cdot E_{teor} + 0{,}195$	$E_{exp} = 0{,}987 \cdot E_{teor} + 0{,}067$
R	0,944	0,936

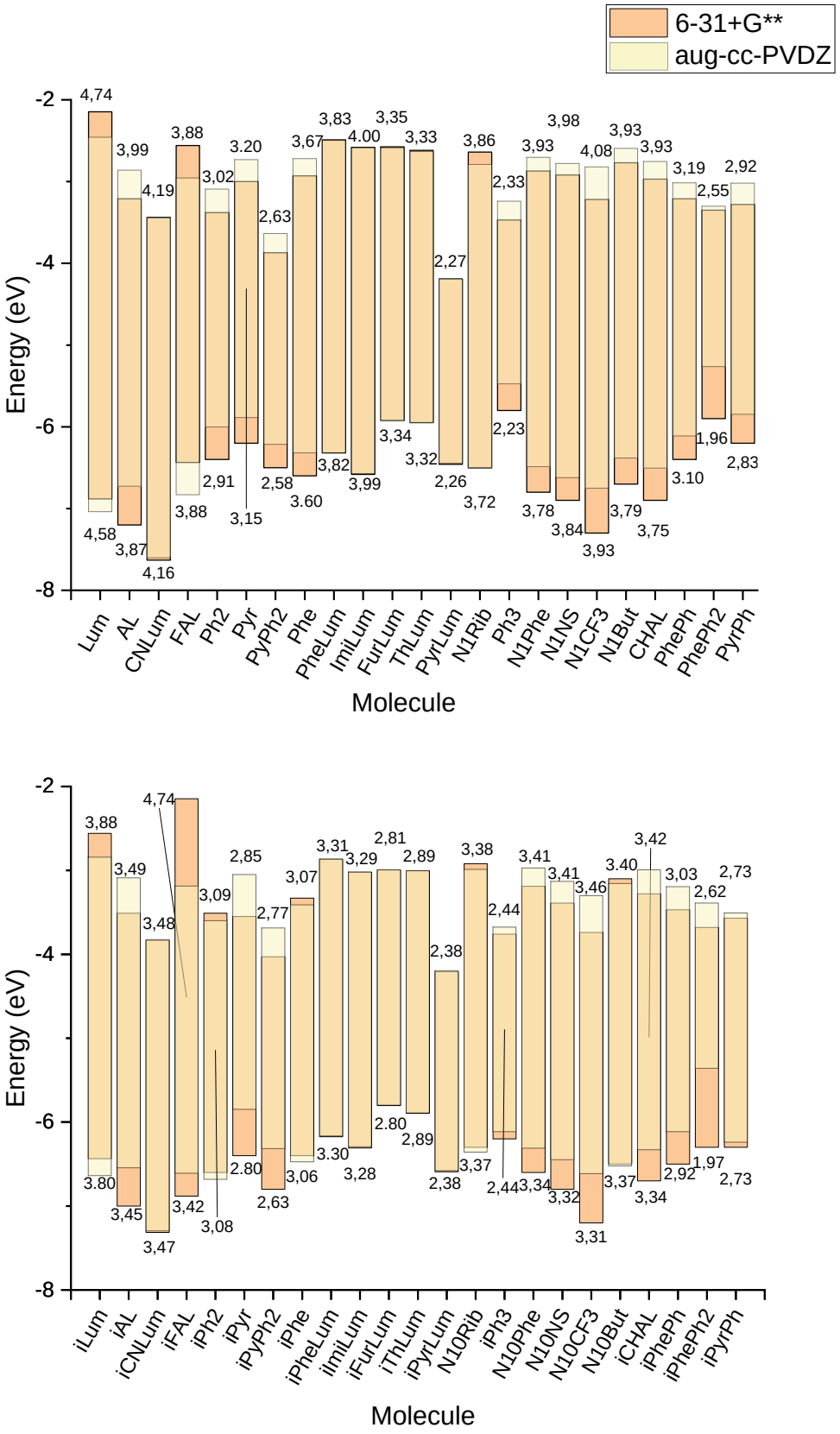

Fig. 8 *The HOMO and LUMO energy levels and associated gaps of the molecules in this study. Values gained from the aug-cc-PVDZ set are shown as semitransparent, values from the 6-31+G** set are in solid colours. HOMO/LUMO Gap values of 6-31+G** are on the top, values from aug-cc-PVDZ are on the bottom of the columns.*

5.2 Adamantylated Polythiophene Building Blocks

For the *syn*-conformers, helical structure is predicted, while the anti-conformers take on a bow-like shape of the backbone, especially prominent in the adamantyl-substituted molecules. The exceptions are **(EDOT)$_8$** and **(PT)$_8$** octamers, which have a practically planar optimized conformation starting from both *syn*- and *anti*- orientations. The *anti*-conformation is slightly energetically preferred, even for extremely large substituents like in the **(ETAT)$_8$** molecule. Further, the differences in energy between the conformers increase with the size of the substituents, as they are of the same order of magnitude for **(PT)$_8$** and **(3HT)$_8$**, and three orders of magnitude larger for the bulky substituents.

Further, it seems that a large, branched substituent, represented by **(MPT)$_8$**, creates a chaotic structure around the backbone, where we cannot consistently expect favourable packing. On the other hand, the addition of an extremely large 3D substituent, like in **(ETAT)$_8$**, causes a torsional strain in the whole structure due to steric repulsion between the individual substituents, evidenced by the large variation on the **(ETAT)$_8$-a** dihedral angles. Further, the methyladamantyl substitution has a similar effect, causing a strain on the backbone due to the proximity of the bulky group, which may have a negative effect on the conjugation and therefore the optical and electronic properties.

With regards to experiment, the dihedrals found for **(T)$_8$** and **(3HT)$_8$** are overestimated [68]. The same is the case for the 1,3,4,6-hexyl substituted sexithiophene [69], although the comparison with **(3HT)$_8$** is not exactly possible – the experimental sexithiophene is not substituted on all rings, which will surely increase the rotational freedom of the hexamer. Further, the gas-phase optimised length of the hexyl side chain was found to be 7.32 Å, while the X-Ray diffraction experiments give the value of 7.70 Å [70] for **P3HT**, which is probably the result of inter-chain interactions in the crystal, which lead to the planarization of the experimentally studied polymers and oligomers.

Next, the side-chain conformations were studied on trimer building blocks – the **(3HT)$_3$**, **(MAT)$_3$**, and **(EAT)$_3$**. The potential energy profiles are shown in **Fig. 9**, together with the relevant dihedral angles. For the model **(3HT)$_3$** chain, a global minimum was found at 280°. Further, rotation is allowed in the range of 0° to 100° with respect to the thiophene ring, with a small torsion barrier at 60°. Furthermore **Fig. 9 (d)** shows the torsional energy with respect to the ethyl bridge between thiophene and the adamantyl substituent, with a clear minimum at 180°. The potential curves are mirrored in the ethyladamantyl substituted molecules since the side chains prefer a conformation, where both hydrogens on the ethyl C(22) and C(23) atoms are equidistant to the S(36) sulphur atom. This happens at 280° in the *syn*- conformer, and at 80° in the *anti*-conformer. It seems that the side chains of **MAT** are restricted in rotation, while the **EAT** chain possesses rigid ethyladamantyl groups with a 180 ° dihedral around the ethyl bridge, which relatively freely rotate with respect to the thiophene moiety. These results agree with previous molecular dynamics studies and crystal structures of **P3HT** [71].

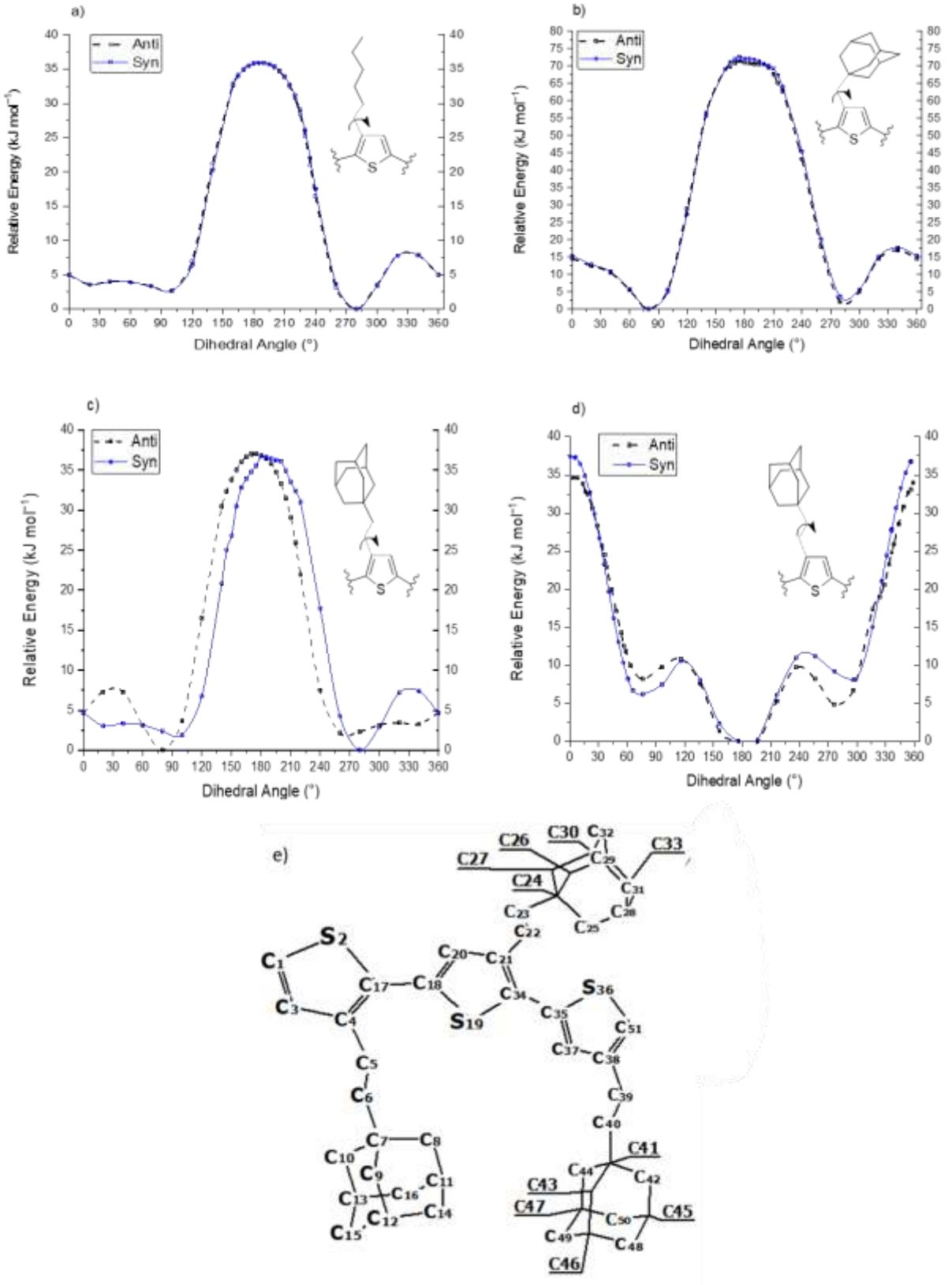

Fig. 9 *The change of relative B3LYP/def2svp energy of single substituent rotation with respect to the indicated torsional angle of the linkage between the thiophene plane and the substituent for model 3-hexylthiophene (a) and 3-methyladamantylthiophene (b) trimers.*

The **MAT** especially has very few stable conformations and steep energetic barriers and thus has the highest chance to create a highly organized structure in comparison to **3HT**. So, although it is not possible to predict the crystal structures exactly, it seems that the **PEAT** should have a slightly higher degree of crystallinity than **P3HT**, and **PMAT** should be significantly better. This arrangement could in turn support the semiconducting properties due to the enhanced packing.

Indeed, as found by the AFM scans shown in **Fig. 10**, the samples show noticeable large structures, that are significantly taller than the rest of the surface (rendered in white). These tall clusters could be impurities left behind from the synthesis but may contain at least some polymer chains. Further, there are visible domains in all the samples that could be crystalline clusters. In **P3HT**, they are around 0.5 μm across and 0.1 μm thick and spaced far apart in a noisy matrix. In **PEAT**, the surface seems to have less noise, and the domains are around 0.5 μm in both directions, rising by a few nm from the matrix, which is rendered in dark orange. The **PMAT** sample contains many domains that are around 0.5 μm in both directions, and they take up most of the surface. This gives some evidence of the increased degree of crystallinity of the adamantyl-substituted polymers. Finally, grooves are found on the surfaces, depicted as black lines, which are likely a product of the thin layer preparation.

This is supported by the Grazing Incidence Wide Angle X-Ray Scattering (GIWAXS) measurement, has revealed edge-on oriented intermolecular packing features with an intramolecular periodicity comparable to **P3HT**, and about double crystal stacking periodicity in the other directions. Overall, the **PMAT** sample was found to have the most ordered structure [JT3]. Next, the optical absorption and emission were investigated, along with the computed electronic transitions and orbital energies. In all cases, only one significant transition was found, the $S_0 \rightarrow S_1$, from the HOMO to the LUMO. A comparison of theoretical transitions with experimental results is shown in **Tab. 3**. Since the experiments were performed in chloroform solution and thin layer, the results are accordingly marked.

The theoretical absorptions of the new molecules are significantly dependent on the conformation, unlike the previously synthesized counterparts. The **(MAT)$_8$** has the best agreement between theory and experiment, where the *anti*-conformer fits the measurements better both in solution and in thin layer. Indeed, it is unlikely that a crystal structure comparable to **P3HT** would contain the helical structures found in the *syn*-derivates. It should also be noted that there is essentially no change in the **PMAT** spectra in the solution and thin layer, likely due to the structural rigidity of the methyladamantyl moiety. On the other hand, the **(3HT)$_8$** and **(EAT)$_8$** have a comparable agreement with experimental values, as both are about 40 nm off. The **(EAT)$_8$-s** variant is closer to experimental data, although it is unlikely that such structures would be present, as discussed before. The **PEAT** sample, however, has a longer effective conjugation compared to **PMAT**, evidenced by the higher absorption wavelength, which should give it better charge transfer properties. Indeed, **PEAT** was shown to have an order of magnitude larger charge carrier mobility than **PMAT**. These findings illustrate the influence of the side chain geometry on optical properties.

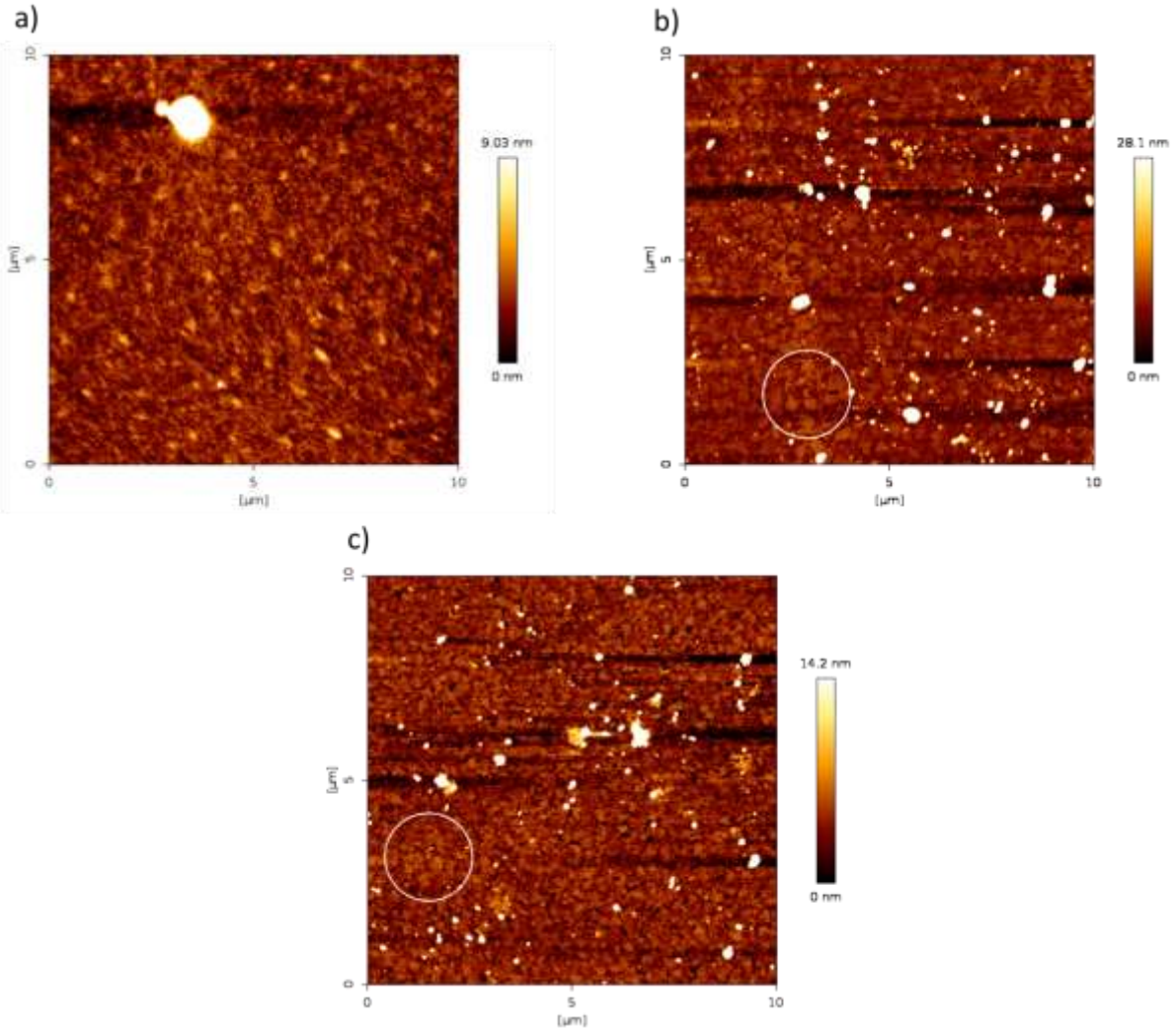

Fig. 10 *the AFM scans of (a)* ***P3HT****; (b)* ***PEAT****; (c)* ***PMAT****; the large clusters are rendered in white, the crystalline domains are circled*

Tab. 3 *The theoretical $S_0 \rightarrow S_1$ transitions of the model octamers, compared with experimental absorption wavelengths where applicable; sol. denotes measurement in chloroform solution, layer denotes results from thin layer measurements.*

Molecule	Theoretical energy (eV)	Theoretical wavelength (nm)	Theoretical oscillator strength	Experimental wavelength (nm)
HT-s	3.050	406	2.61	450 sol.
HT-a	3.050	406	2.61	508 layer
MAT-s	3.025	409	2.48	390 sol.
MAT-a	3.215	385	2.36	387 layer
EAT-s	2.933	422	2.46	458 sol.
EAT-a	3.094	400	2.49	475 layer

The frontier molecular orbital energies are shown in **Fig. 11**. The *syn*- and *anti*-conformations have no influence on the energy levels of **(T)$_8$** and **(3HT)$_8$**, and the HOMO/LUMO gap is lower for the *syn*-forms of the other molecules, which is consistent with the electronic excitation predictions. The values are slightly larger in **(MAT)$_8$**, documenting the larger influence of the adamantyl when it is closer to the backbone. The polymer limit of the **P3HT** HOMO/LUMO gap is around 2.50 eV [17], indicating that these oligomers do not reach it. The situation is likely the same for **(EAT)$_8$** as the predicted absorption wavelength is considerably lower than the experimental value, indicating that the predicted excitation energy is larger than it truly is.

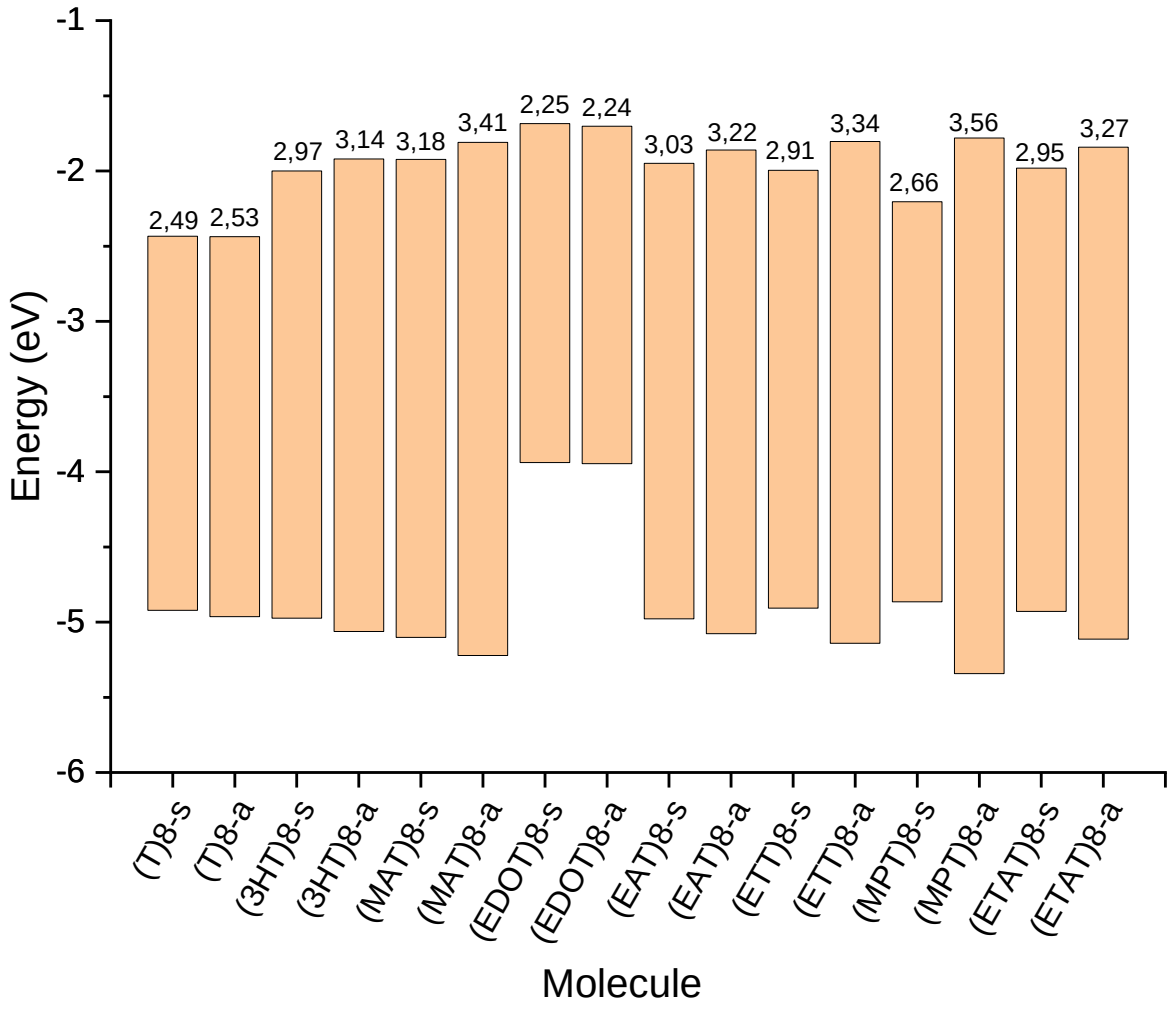

Fig. 11 *The theoretical frontier molecular orbital energies and the HOMO/LUMO gap values of the model octamers*

Finally, the novel polymers possess the thermal and chemical stability to produce long-lived devices and are processable in solvents convenient for upscaling and industrial production, such as chloroform [JT3]. The adamantane side chains have proved to provide a good amount of space for intermolecular interactions and the insertion of the side substituents of a neighbouring chain, showing a crystal structure comparable to **P3HT**. Thus, these materials could be serious competitors in the future.

6 CONCLUSION

For the flavin molecules, several basis sets were tested in combination with the B3LYP functional to see which has the best fit to experimental electronic spectra. Interestingly, the def2SVP basis set was found to be accurate but not precise, being the closest to a 1:1 correlation, but with a larger spread of individual values. On the other hand, the 6-31+G** and aug-cc-PVDZ sets overestimate many transitions but have an overall better correlation. A common flaw is the inaccuracy concerning the isoalloxazine and isolumazine $S_0 \rightarrow S_1$ absorption peak. Indeed, if these isomeric forms are excluded, the fit is significantly better. This also represents room for improvement of the computational model. Nevertheless, the B3LYP/6-31+G** method represents a cost-effective and accurate way of computing electronic spectra.

Briefly, the flavin structure was investigated. The modifications considered in this work were found to generally distort the alloxazine and lumazine moieties and lower their aromaticity. The geometry of lumazines substituted with freely rotating rings was found to be strongly dependent on the N(1) to N(8) isomerization, and a bend of the alloxazine moiety was found for N(10) substituted molecules as previously reported. A larger impact of electron-withdrawing substituents on the **Lum** molecule compared to **AL** was found. This is likely caused by the shielding of the substituent by the additional benzene ring of **AL**. From this point of view, the better synthetic strategy seems to be using electron-withdrawing or donating substituents to modify **Lum**, while fusing aromatic rings to **AL**, to tune the energy levels and absorption spectra. Synthesis of new derivatives according to the theoretical investigation is ongoing.

The novel polythiophene molecules were found to have optoelectronic properties like **P3HT**, with molecular packing that seems to agree with the shape of the computed *anti*-conformers of the model octamers in question. The analysis of side chain conformations has found the methyladamantyl substituted chains to have a more rigid structure, due to having fewer degrees of freedom than ethyladamantyl chains. With later AFM and crystallographic analysis, the **PMAT** sample was indeed found to have a higher degree of crystallinity than **PEAT**. Since the conductivity of polythiophenes stems mainly from molecular packing, it is interesting to note that the **PEAT** sample was found to have a larger charge carrier mobility than **PMAT**, although a theoretical explanation for this would likely require a molecular dynamics treatment.

In the future, the models could be improved by the use of molecular dynamics models, to better study the conformations and molecular packing of both flavins and polythiophenes in the solid state, bringing more accurate predictions and a better understanding of the charge transfer processes involved. Experimentally, more attention could be paid to the interactions of flavins with water and other solvents, especially in the case of such molecules as **CNLum** and **FAL**, where the interaction of the exposed electron-withdrawing groups with polar solvent molecules could have interesting effects. A publication focused on this topic is currently in preparation. As far as polythiophenes are concerned, more attention could be paid to the modifications of the polymer backbone, and detailed studies of adiabatic ionization potentials, electron affinities and reorganization energies will have to be carried out to gain a truly deep understanding of the effects of both side substitution and backbone modification.

7 REFERENCES

[1] RAJENDAR, Burki, Arivazhagan RAJENDRAN, Zhiqiang YE, Eriko KANAI, Yusuke SATO, Seiichi NISHIZAWA, Marek SIKORSKI and Norio TERAMAE. Effect of substituents of alloxazine derivatives on the selectivity and affinity for adenine in AP-site-containing DNA duplexes. *Organic & Biomolecular Chemistry* [online]. 2010, **8**(21) [accessed on 2022-02-21]. ISSN 1477-0520. doi:10.1039/c0ob00057d

[2] LEWARS, Errol G. *Computational Chemistry: Introduction to the Theory and Applications of Molecular and Quantum Mechanics*. 2nd. Springer Netherlands, 2011. ISBN 978-90-481-3861-6.

[3] LEVINE, Ira N. *Quantum chemistry*. 7th ed. Boston: Pearson, c2014. ISBN 978-0-321-80345-0.

[4] DITCHFIELD, R., W. J. HEHRE and J. A. POPLE. Self-Consistent Molecular-Orbital Methods. IX. An Extended Gaussian-Type Basis for Molecular-Orbital Studies of Organic Molecules. The Journal of Chemical Physics [online]. 1971, 54(2), 724-728 [accessed 2022-09-05]. ISSN 0021-9606. Available from: doi:10.1063/1.1674902

[5] MCLEAN, A. D. and G. S. CHANDLER. Contracted Gaussian basis sets for molecular calculations. I. Second row atoms, Z =11–18. The Journal of Chemical Physics [online]. 1980, 72(10), 5639-5648 [accessed 2022-09-05]. ISSN 0021-9606. Available from: doi:10.1063/1.438980

[6] WEIGEND, Florian and Reinhart AHLRICHS. Balanced basis sets of split valence, triple zeta valence and quadruple zeta valence quality for H to Rn: Design and assessment of accuracy. Physical Chemistry Chemical Physics [online]. 2005, 7(18) [accessed 2022-09-05]. ISSN 1463-9076. Available from: doi:10.1039/b508541a

[7] JENSEN, Frank. *Introduction to computational chemistry*. Third edition. Chichester: Wiley, 2017. ISBN 978-111-8825-990.

[8] DUNNING, Thom H. Gaussian basis sets for use in correlated molecular calculations. I. The atoms boron through neon and hydrogen. The Journal of Chemical Physics [online]. 1989, 90(2), 1007-1023 [accessed 2022-09-05]. ISSN 0021-9606. Available from: doi:10.1063/1.456153

[9] ULLRICH, Carsten A. Time-dependent density-functional theory: concepts and applications. Oxford: Oxford University Press, 2012. Oxford graduate texts. ISBN 978-0-19-956302-9.

[10] DREUW, Andreas and Martin HEAD-GORDON. Failure of Time-Dependent Density Functional Theory for Long-Range Charge-Transfer Excited States: The Zincbacteriochlorin−Bacteriochlorin and Bacteriochlorophyll−Spheroidene Complexes. Journal of the American Chemical Society [online]. 2004, 126(12), 4007-4016 [accessed 2022-09-05]. ISSN 0002-7863. Available from: doi:10.1021/ja039556n

[11] HAILE, J.M. *Molecular Dynamics Simulation: Elementary Methods*. New York: John Wiley, 1992. ISBN 0-471-81966-2.

[12] LUKEŠ, Vladimír, Viliam LAURINC, Michal ILČIN and Erik KLEIN. *Počítačové modelovanie molekúl: Metódy počítačovej chémie*. Bratislava: Nakladateľstvo STU, 2011. ISBN 978-80-227-3456-1.

[13] KATRITZKY, Alan R., Karl JUG and Daniela C. ONICIU. Quantitative Measures of Aromaticity for Mono-, Bi-, and Tricyclic Penta- and Hexaatomic Heteroaromatic Ring Systems and Their Interrelationships. Chemical Reviews [online]. 2001, 101(5), 1421-1450 [accessed 2020-04-28]. DOI: 10.1021/cr990327m. ISSN 0009-2665. Available from: https://pubs.acs.org/doi/10.1021/cr990327m

[14] MERZ, Thomas, Genaro BIERHANCE, Ernst-Christian FLACH, et.al. Description of excited states in photochemistry with theoretical methods. *Physical Sciences Reviews* [online]. 2021, **6**(3) [accessed 2022-03-28]. ISSN 2365-659X. Available from: doi:10.1515/psr-2017-0178

[15] OTERO, R., A.L. VÁZQUEZ DE PARGA and J.M. GALLEGO. Electronic, structural and chemical effects of charge-transfer at organic/inorganic interfaces. Surface Science Reports [online]. 2017, 72(3), 105-145 [accessed 2022-09-05]. ISSN 01675729. Available from: doi:10.1016/j.surfrep.2017.03.001

[16] RAPTA, Peter, LUKEŠ, Vladimír, Viliam LAURINC, Michal ILČIN and Erik KLEIN. Organické materiály pro elektroniku, Optoelektroniku a senzoriku; Aplikace moderných. ISBN 978-80-227-3617-6.

[17] BHATTA, Ram S. and Mesfin TSIGE. Chain length and torsional dependence of exciton binding energies in P3HT and PTB7 conjugated polymers: A first-principles study. Polymer [online]. 2014, 55(11), 2667-2672 [accessed. 2022-09-05]. ISSN 00323861. Available from: doi:10.1016/j.polymer.2014.04.022

[18] GIERSCHNER, J., J. CORNIL and H.-J. EGELHAAF. Optical Bandgaps of π-Conjugated Organic Materials at the Polymer Limit: Experiment and Theory. Advanced Materials [online]. 2007, 19(2), 173-191 [accessed 2022-09-05]. ISSN 09359648. Available from: doi:10.1002/adma.200600277

[19] KUHN, Hans. A Quantum-Mechanical Theory of Light Absorption of Organic Dyes and Similar Compounds. The Journal of Chemical Physics [online]. 1949, 17(12), 1198-1212 [accessed 2022-09-05]. ISSN 0021-9606. Available from: doi:10.1063/1.1747143

[20] WYKES, Michael, Begoña MILIÁN-MEDINA and Johannes GIERSCHNER. Computational engineering of low bandgap copolymers. Frontiers in Chemistry [online]. 2013, 1 [accessed 2022-09-05]. ISSN 2296-2646. Available from: doi:10.3389/fchem.2013.00035

[21] CIBULKA, Radek and Marco W. FRAAIJE, ed. Flavin-Based Catalysis: Principles and Applications. 1. Weinheim: Wiley-VCH, 2021. ISBN 978-3-527-34834-3.

[22] KLEIN, R. and I. TATISCHEFF. TAUTOMERISM AND FLUORESCENCE OF LUMAZINE. Photochemistry and Photobiology [online]. 1987, 45(1), 55-65 [accessed 2022-02-18]. ISSN 0031-8655. Available from: doi:10.1111/j.1751-1097.1987.tb08405.x

[23] GOLCZAK, Anna, Małgorzata INSIŃSKA-RAK, Amirali DAVOUDPOUR, et al. Photophysical properties of alloxazine derivatives with extended aromaticity – Potential redox-sensitive fluorescent probe. Spectrochimica Acta Part A: Molecular and Biomolecular Spectroscopy [online]. 2022, 272 [accessed 2022-09-07]. ISSN 13861425. Available from: doi:10.1016/j.saa.2022.120985

[24] KIS, Klaus, Rainer VOLK and Adelbert BACHER. Biosynthesis of Riboflavin. Studies on the Reaction Mechanism of 6,7-Dimethyl-8-ribityllumazine Synthase. Biochemistry [online]. 1995, 34(9), 2883-2892 [accessed 2022-09-06]. ISSN 0006-2960. Available from: doi:10.1021/bi00009a019

[25] YOSHIMOTO, Satoshi, Nana KOHARA, Natsu SATO, et. al. Riboflavin Plays a Pivotal Role in the UVA-Induced Cytotoxicity of Fibroblasts as a Key Molecule in the Production of H2O2 by UVA Radiation in Collaboration with Amino Acids and Vitamins. International Journal of Molecular Sciences [online]. 2020, 21(2) [accessed 2022-09-07]. ISSN 1422-0067. Available from: doi:10.3390/ijms21020554

[26] GUO, Huimin, Hongyu XIA, Xiaolin MA, et. al. Efficient Photooxidation of Sulfides with Amidated Alloxazines as Heavy-atom-free Photosensitizers. ACS Omega [online]. 2020, 5(18), 10586-10595 [accessed. 2022-09-07]. ISSN 2470-1343. Available from: doi:10.1021/acsomega.0c01087

[27] MAL, Madhushree and Debabrata MANDAL. Solvent and pH-sensitive Fluorescence Response of Alloxazine. Journal of Photochemistry and Photobiology A: Chemistry [online]. 2021, 404 [accessed 2022-02-18]. ISSN 10106030. Available from: doi:10.1016/j.jphotochem.2020.112888

[28] RICHTAR, Jan, Patricie HEINRICHOVA, Dogukan APAYDIN, et al. Novel Riboflavin-Inspired Conjugated Bio-Organic Semiconductors. Molecules [online]. 2018, 23(9) [accessed 2022-02-21]. ISSN 1420-3049 Available from: doi:10.3390/molecules23092271

[29] MOYON, N. Shaemningwar and Sivaprasad MITRA. Fluorescence Solvatochromism in Lumichrome and Excited-State Tautomerization: A Combined Experimental and DFT Study. The Journal of Physical Chemistry A [online]. 2011, 115(12), 2456-2464 [accessed 2022-09-07]. ISSN 1089-5639. Available from: doi:10.1021/jp1102687

[30] DENOFRIO, M. Paula, Andrés H. THOMAS, André M. BRAUN, et. al. Photochemical and photophysical properties of lumazine in aqueous solutions. Journal of Photochemistry and Photobiology

A: Chemistry [online]. 2008, 200(2-3), 282-286 [accessed 2022-09-07]. ISSN 10106030. Available from: doi:10.1016/j.jphotochem.2008.08.003

[31] AFANEH, Akef T. and Georg SCHRECKENBACH. Conformation/Tautomerization effect on the pK a values of lumazine and 6-thienyllumazine. Journal of Physical Organic Chemistry [online]. 2014, 27(8), 690-700 [accessed 2022-09-07]. ISSN 08943230. Available from: doi:10.1002/poc.3320

[32] WÖRNER, Jakob, Jing CHEN, Adelbert BACHER and Stefan WEBER. Non-classical disproportionation revealed by photo-chemically induced dynamic nuclear polarization NMR. Magnetic Resonance [online]. 2021, 2(1), 281-290 [accessed 2022-09-07]. ISSN 2699-0016. Available from: doi:10.5194/mr-2-281-2021

[33] DUTTA CHOUDHURY, Sharmistha and Haridas PAL. Intriguing Tautomerism of Lumichrome in Binary Aqueous Solvent Mixtures: Implications for Probing Microenvironments. The Journal of Physical Chemistry B [online]. 2016, 120(46), 11970-11977 [accessed 2022-09-07]. ISSN 1520-6106. Available from: doi:10.1021/acs.jpcb.6b08777

[34] KHATTAB, Muhammad, Feng WANG and Andrew H. A. CLAYTON. Micro-solvation of tyrosine-kinase inhibitor AG1478 explored with fluorescence spectroscopy and computational chemistry. RSC Advances [online]. 2017, 7(50), 31725-31735 [accessed 2022-09-07]. ISSN 2046-2069. Available from: doi:10.1039/C7RA04435F

[35] SALZMANN, Susanne and Christel M. MARIAN. The photophysics of alloxazine: a quantum chemical investigation in vacuum and solution. Photochemical & Photobiological Sciences [online]. 2009, 8(12) [accessed 2022-09-07]. ISSN 1474-905X. Available from: doi:10.1039/b9pp00022d

[36] SIKORSKA, Ewa, Igor V. KHMELINSKII, David R. WORRALL, et. al. Spectroscopy and Photophysics of Iso- and Alloxazines: Experimental and Theoretical Study. Journal of Fluorescence [online]. 2004, 14(1), 57-64 [accessed 2022-09-07]. ISSN 1053-0509. Available from: doi:10.1023/B:JOFL.0000014660.59105.31

[37] SIKORSKA, Ewa, Igor V KHMELINSKII, Siân L WILLIAMS, et. al. Spectroscopy and photophysics of 6,7-dimethyl-alloxazine: experimental and theoretical study. Journal of Molecular Structure [online]. 2004, 697(1-3), 199-205 [accessed 2022-09-07]. ISSN 00222860. Available from: doi:10.1016/j.molstruc.2004.04.011

[38] MAL, Madhushree and Debabrata MANDAL. Phototautomerism of Alloxazine in Acetic acid – Water solvent systems. Journal of Molecular Liquids [online]. 2021, 322 [accessed 2022-09-07]. ISSN 01677322. Available from: doi:10.1016/j.molliq.2020.114928

[39] PENZKOFER, Alfons. Absorption and emission spectroscopic investigation of alloxazine in aqueous solutions and comparison with lumichrome. Journal of Photochemistry and Photobiology A: Chemistry [online]. 2016, 314, 114-124 [accessed 2022-09-07]. ISSN 10106030. Available from: doi:10.1016/j.jphotochem.2015.08.011

[40] NORTH, Michael A., Sudeep BHATTACHARYYA and Donald G. TRUHLAR. Improved Density Functional Description of the Electrochemistry and Structure−Property Descriptors of Substituted Flavins. The Journal of Physical Chemistry B [online]. 2010, 114(46), 14907-14915 [accessed 2022-09-07]. ISSN 1520-6106. Available from: doi:10.1021/jp108024b

[41] ABBAS, Zina A. A., Najwa M. J. ABU-MEJDAD, et. al. Synthesis and Biological Evaluation of New Dipyridylpteridines, Lumazines, and Related Analogues. Journal of Heterocyclic Chemistry [online]. 2017, 54(2), 895-903 [accessed 2022-09-07]. ISSN 0022152X. Available from: doi:10.1002/jhet.2651

[42] SAKAI, Ken-ichi, Kenta NAGAHARA, Yuuya YOSHII, et. al. Structural and Spectroscopic Study of 6,7-Dicyano-Substituted Lumazine with High Electron Affinity and Proton Acidity. The Journal of Physical Chemistry A [online]. 2013, 117(17), 3614-3624 [accessed 2022-09-07]. ISSN 1089-5639. Available from: doi:10.1021/jp401528c

[43] TURKOGLU, Gulsen, M. Emin CINAR and Turan OZTURK. Thiophene-Based Organic Semiconductors. Topics in Current Chemistry [online]. 2017, 375(6) [accessed 2022-09-07]. ISSN 2365-0869. Available from: doi:10.1007/s41061-017-0174-z

[44] HALIK, Marcus, Hagen KLAUK, Ute ZSCHIESCHANG, et. al. High-mobility organic thin-film transistors based on α,α ′ -didecyloligothiophenes. Journal of Applied Physics [online]. 2003, 93(5), 2977-2981 [accessed 2022-09-07]. ISSN 0021-8979. Available from: doi:10.1063/1.1543246

[45] CAO, Zhiqiang, Luke GALUSKA, Zhiyuan QIAN, et al. The effect of side-chain branch position on the thermal properties of poly(3-alkylthiophenes). Polymer Chemistry [online]. 2020, 11(2), 517-526 [accessed 2022-09-07]. ISSN 1759-9954. Available from: doi:10.1039/C9PY01026B

[46] SCHAFFRINNA, Roy and Martina SCHWAGER. Effect of interchain interactions on the optical characteristics of polythiophene derivatives. Materials Research Innovations [online]. 2021, 25(1), 23-28 [accessed 2022-09-07]. ISSN 1432-8917. Available from: doi:10.1080/14328917.2020.1728485

[47] KLEINSCHMIDT, Andrew T., Samuel E. ROOT and Darren J. LIPOMI. Poly(3-hexylthiophene) (P3HT): fruit fly or outlier in organic solar cell research?. Journal of Materials Chemistry A [online]. 2017, 5(23), 11396-11400 [accessed 2022-09-07]. ISSN 2050-7488. Available from: doi:10.1039/C6TA08317J

[48] NGUYEN, Thanh-Danh, Van-Hai NGUYEN, Jongwoo SONG, et. al. Molecular Weight-Dependent Physical and Photovoltaic Properties of Poly(3-alkylthiophene)s with Butyl, Hexyl, and Octyl Side-Chains. Polymers [online]. 2021, 13(19) [accessed 2022-09-07]. ISSN 2073-4360. Available from: doi:10.3390/polym13193440

[49] KRAJČOVIČ, Jozef, Alexander KOVALENKO, Patricie HEINRICHOVÁ, et. al. Adamantyl side groups boosting the efficiency and thermal stability of organic solid-state fluorescent dyes. Journal of Luminescence [online]. 2016, 175, 94-99 [accessed 2022-09-07]. ISSN 00222313. Available from: doi:10.1016/j.jlumin.2016.02.019

[50] MARCON, Valentina and Guido RAOS. Molecular Modeling of Crystalline Oligothiophenes: Testing and Development of Improved Force Fields. The Journal of Physical Chemistry B [online]. 2004, 108(46), 18053-18064 [accessed 2022-09-07]. ISSN 1520-6106. Available from: doi:10.1021/jp047128d

[51] DARLING, Seth B. and Michael STERNBERG. Importance of Side Chains and Backbone Length in Defect Modeling of Poly(3-alkylthiophenes). The Journal of Physical Chemistry B [online]. 2009, 113(18), 6215-6218 [accessed 2022-09-07]. ISSN 1520-6106. Available from: doi:10.1021/jp808045j

[52] SCHILINSKY, Pavel, Udom ASAWAPIROM, Ullrich SCHERF, et. al. Influence of the Molecular Weight of Poly(3-hexylthiophene) on the Performance of Bulk Heterojunction Solar Cells. Chemistry of Materials [online]. 2005, 17(8), 2175-2180 [accessed 2022-09-07]. ISSN 0897-4756. Available from: doi:10.1021/cm047811c

[53] HOSSAIN, Mohammad S., Cuong Q. LE, Ebenezer JOSEPH, et. al. Convenient synthesis of deazaflavin cofactor FO and its activity in F 420 -dependent NADP reductase. Organic & Biomolecular Chemistry [online]. 2015, 13(18), 5082-5085 [accessed 2022-09-07]. ISSN 1477-0520. Available from: doi:10.1039/C5OB00365B

[54] LEE, Chengteh, Weitao YANG and Robert G. PARR. Development of the Colle-Salvetti correlation-energy formula into a functional of the electron density. Physical Review B [online]. 1988, 37(2), 785-789 [accessed 2022-09-07]. ISSN 0163-1829. Available from: doi:10.1103/PhysRevB.37.785

[55] DUNNING, Thom H. Gaussian basis sets for use in correlated molecular calculations. I. The atoms boron through neon and hydrogen. The Journal of Chemical Physics [online]. 1989, 90(2), 1007-1023 [accessed 2022-09-07]. ISSN 0021-9606. Available from: doi:10.1063/1.456153

[56] WEIGEND, Florian and Reinhart AHLRICHS. Balanced basis sets of split valence, triple zeta valence and quadruple zeta valence quality for H to Rn: Design and assessment of accuracy. Physical Chemistry Chemical Physics [online]. 2005, 7(18) [accessed 2022-09-07]. ISSN 1463-9076. Available from: doi:10.1039/b508541a

[57] CARICATO, Marco. Absorption and Emission Spectra of Solvated Molecules with the EOM–CCSD–PCM Method. Journal of Chemical Theory and Computation [online]. 2012, 8(11), 4494-4502 [accessed 2022-09-07]. ISSN 1549-9618. Available from: doi:10.1021/ct3006997

[58] BOUZZINE, Si Mohamed, Saïd BOUZAKRAOUI, Mohammed BOUACHRINE and Mohamed HAMIDI. Density functional theory (B3LYP/6-31G*) study of oligothiophenes in their aromatic and polaronic states. Journal of Molecular Structure: THEOCHEM [online]. 2005, 726(1-3), 271-276 [accessed 2022-09-07]. ISSN 01661280. Available from: doi:10.1016/j.theochem.2005.04.023

[59] Dimethyl sulfoxide|51779. Honeywell Research Chemicals [online]. Honeywell International, 2022 [accessed 2022-09-07]. Available from: https://lab.honeywell.com/shop/dimethyl-sulfoxide-51779

[60] Dimethyl Sulfoxide. Penta Chemicals [online]. Praha: PENTA, 2020 [cit. 2022-09-09]. Dostupné z: https://www.pentachemicals.eu/en/chemicals/dimethyl-sulfoxide-69

[61] M. J. Frisch, G. W. Trucks, H. B. Schlegel, G. E. Scuseria, M. A. Robb, J. R. Cheeseman, G. Scalmani, V. Barone, G. A. Petersson, H. Nakatsuji, X. Li, M. Caricato, A. V. Marenich, J. Bloino, B. G. Janesko, R. Gomperts, B. Mennucci, H. P. Hratchian, J. V. Ortiz, A. F. Izmaylov, J. L. Sonnenberg, D. Williams-Young, F. Ding, F. Lipparini, F. Egidi, J. Goings, B. Peng, A. Petrone, T. Henderson, D. Ranasinghe, V. G. Zakrzewski, J. Gao, N. Rega, G. Zheng, W. Liang, M. Hada, M. Ehara, K. Toyota, R. Fukuda, J. Hasegawa, M. Ishida, T. Nakajima, Y. Honda, O. Kitao, H. Nakai, T. Vreven, K. Throssell, J. A. Montgomery, Jr., J. E. Peralta, F. Ogliaro, M. J. Bearpark, J. J. Heyd, E. N. Brothers, K. N. Kudin, V. N. Staroverov, T. A. Keith, R. Kobayashi, J. Normand, K. Raghavachari, A. P. Rendell, J. C. Burant, S. S. Iyengar, J. Tomasi, M. Cossi, J. M. Millam, M. Klene, C. Adamo, R. Cammi, J. W. Ochterski, R. L. Martin, K. Morokuma, O. Farkas, J. B. Foresman, and D. J. Fox, Gaussian, Inc., Wallingford CT, 2016.

[62] Analytik Jena GmbH. ASpect UV Software, Jena, Germany, 2020.

[63] Horiba Instruments Incorporated, FluorEssence Software, Minami-ku Kyoto, Japan, 2019.

[64] MetaCentrum [online]. Praha: MetaCentrum, VO, 2022 [accessed 2022-09-07]. Available from: https://metavo.metacentrum.cz/en/index.html

[65] Hanwell, M.; Curtis, D. E.; Lonie, D. C.; Vandermeersch, T.; Zurek, E.; Hutchinson, G. R. Avogadro: An advanced semantic chemical editor, visualization, and analysis platform. J Cheminform 2012 4.

[66] Flukiger P, Luthi HP, Sortmann S, Weber J. Molekel 4.3 (2002), Swiss National Supercomputing Centre, Manno, Switzerland.

[67] CHANG, Xue-Ping, Xiao-Ying XIE, Shi-Yun LIN and Ganglong CUI. QM/MM Study on Mechanistic Photophysics of Alloxazine Chromophore in Aqueous Solution. The Journal of Physical Chemistry A [online]. 2016, 120(31), 6129-6136 [accessed 2022-09-07]. ISSN 1089-5639. Available from: doi:10.1021/acs.jpca.6b02669

[68] HOROWITZ, Gilles, Bernard BACHET, Abderrahim YASSAR, et. al. Growth and Characterization of Sexithiophene Single Crystals. Chemistry of Materials [online]. 1995, 7(7), 1337-1341 [accessed 2022-09-07]. ISSN 0897-4756. Available from: doi:10.1021/cm00055a010

[69] NEUMANN, Marcus A., Consiglia TEDESCO, Silvia DESTRI, et. al. Bridging the gap – structure determination of the red polymorph of tetrahexylsexithiophene by Monte Carlo simulated annealing, first-principles DFT calculations and Rietveld refinement. Journal of Applied Crystallography [online]. 2002, 35(3), 296-303 [accessed 2022-09-07]. ISSN 0021-8898. Available from: doi:10.1107/S0021889802002844

[70] PROSA, T. J., M. J. WINOKUR, Jeff MOULTON, et. al. X-ray structural studies of poly(3-alkylthiophenes): an example of an inverse comb. Macromolecules [online]. 1992, 25(17), 4364-4372 [accessed 2022-09-07]. ISSN 0024-9297. Available from: doi:10.1021/ma00043a019

[71] DAG, Sefa and Lin-Wang WANG. Packing Structure of Poly(3-hexylthiophene) Crystal: Ab Initio and Molecular Dynamics Studies. The Journal of Physical Chemistry B [online]. 2010, 114(18), 5997-6000 [accessed 2022-09-07]. ISSN 1520-6106. Available from: doi:10.1021/jp1008219

8 CURRICULUM VITAE

Career to date:
1/9/2021 – 1/8/2022: Faculty of Chemistry BUT
Position: research worker
Job description: performing atomic force microscopy measurements

1/10/2018 – 1/10/2019: Faculty of Chemistry BUT – Materials Research Centre
Position: laboratory technician.
Job description: mathematical modelling of physico-chemical phenomena (e. g. formation of an electric double layer on an electrode-electrolyte boundary), common laboratory work.

1/7/2017 – 31/8/2017: Polymer Institute Brno, branch of Unipetrol RPA, s.r.o.
Position: laboratory technician.
Job description: cleaning and additivation of polyethylene, synthesized on-site, purification of technical alcohol by distillation, common laboratory work.

Education:
10/2019 – 03/2020: Slovak University of Technology in Bratislava, Slovak Republic
Faculty: Faculty of Chemical and Food Technology
ERASMUS+ traineeship: computational chemistry, chemical physics

09/2018 – 11/2022: Brno University of Technology, Czech Republic
Faculty: Faculty of Chemistry
Doctoral programme: Chemistry, technology and properties of materials

09/2013 – 06/2018: Brno University of Technology, Czech Republic
Faculty: Faculty of Chemistry
Bachelor's and master's programme: Chemistry, technology and properties of materials
Branch: Chemistry, technology and properties of materials

9 OVERVIEW OF THE AUTHOR'S PUBLICATIONS

[JT1] Spectroscopic behavior of alloxazine-based dyes with extended aromaticity: Theory vs Experiment.

CAGARDOVÁ, Denisa, **TRUKSA, Jan**, MICHALÍK, Martin, RICHTÁR, Jan, WEITER, Martin, KRAJČOVIČ, Jozef, LUKEŠ Vladimír

In this paper, the large conjugated alloxazines were studied, and the theoretically predicted properties were compared to experimental results. The B3LYP and CAM-B3LYP functionals were used, together with the 6-31+G** basis set. While the range-corrected CAM-B3LYP did not give correct predictions, the B3LYP/6-31+G** method proved to be efficient for the spectroscopic properties' predictions. To the author's knowledge, this was the first scientific paper where systematic theoretical investigations of alloxazines with fused benzene rings was published.

The author's personal contribution

The author ran the theoretical calculations, evaluated the resulting data – e.g. the HOMED indices, and the fit of experimental and theoretical data, and co-authored the manuscript.

[JT2] Theoretical modeling of optical spectra of N(1) and N(10) substituted lumichrome derivatives

CAGARDOVÁ, Denisa, **TRUKSA, Jan**, MICHALÍK, Martin, RICHTÁR, Jan, WEITER, Martin, KRAJČOVIČ, Jozef, LUKEŠ Vladimír

In this paper, the influence of substitutions in the N(1) and N(10) positions of alloxazine on the structure and frontier orbital energies was investigated. The bending of the **iAL** molecule was described, as anticipated in previous literature [North 2010].

The author's personal contribution

The author evaluated the data from theoretical calculations and co-authored the manuscript.

[JT3] Novel Adamantane Substituted Polythiophenes as Competitors to Poly(3-Hexylthiophene)

JANČÍK, Jan, POSPÍŠIL, Jan, KRATOCHVÍL, Matouš, TRUKSA, Jan, ALTAMURA, Davide, GIANNINI, Cinza, WEITER, Martin, BLASI, Davide, LUKEŠ, Vladimír, GŁOWACKI, Eric D., KRAJČOVIČ, Jozef

Here, the novel adamantyl-substituted polythiophene chains were introduced, and the synthesis, purification and characterization were described, including the theoretical study of chain conformations, spectroscopic and electrochemical measurements, crystallography and AFM scanning. These materials were found to have comparable properties to **P3HT**, showing the utility of adamantyl substitutions.

The author's personal contribution

The author performed the conformation analysis of the model oligomers and their theoretical electronic excitations and co-authored this part of the manuscript with prof. Lukeš. Further, the author performed the AFM scans, and authored this part of the manuscript.

9.1 Conference Contributions

TRUKSA, Jan, CAGARDOVÁ, Denisa, MICHALÍK, Martin, RICHTÁR, Jan, WEITER, Martin, KRAJČOVIČ, Jozef, LUKEŠ, Vladimír. Spectroscopic behavior of alloxazine derivates: Theory vs Experiment. DCMS Materials 4.0 Summer School. Book of Abstracts, Dresden 2021 pp.60

TRUKSA, Jan, CAGARDOVÁ, Denisa, MICHALÍK, Martin, RICHTÁR, Jan, WEITER, Martin, KRAJČOVIČ, Jozef, LUKEŠ, Vladimír. Visible-Light Spectroscopy of Alloxazines: Theory and Experiment. 8th Meeting on Chemistry and Life. 2021. Book of abstracts. Brno: Vysoké učení technické v Brně, 2021.

TRUKSA, Jan, CAGARDOVÁ, Denisa, MICHALÍK, Martin, RICHTÁR, Jan, WEITER, Martin, KRAJČOVIČ, Jozef, LUKEŠ, Vladimír. The Effect of Substitution and Aromatic Ring Condensation on the Optical Properties of Alloxazine: a Theoretical Study. CHEMIE JE ŽIVOT 2020 Book of Abstracts. Brno: Vysoké učení technické v Brně, 2020. pp. 225-230. ISBN 978-80-214-5921-2

TRUKSA, Jan, SALYK, Ota. Modelling of Bioelectronic Devices. 7th Meeting on Chemistry and Life 2018. CZECH CHEMICAL SOCIETY SYMPOSIUM SERIES 16 (2018). Asociace Českých Chemických Společností, 2018. p 518-522. ISSN 2336-7210